

## Electrical Supporting information

### Application of sugar-containing biomass: one-step synthesis of 2-furylgyoxylic acid and its derivatives from vitamin C precursor

Jiao Chen,<sup>a</sup> Zhenhua Zhu,<sup>a</sup> Jiali Cai,<sup>b</sup> Mengru Cao,<sup>a</sup> Feng Sha,<sup>c</sup> Sha Tao,<sup>a</sup> Hao Yang,<sup>a</sup> Haifeng Gan,<sup>a</sup> Hongli Wu,<sup>a</sup> Fei Cao,<sup>\*a</sup> Lili Zhao<sup>\*b</sup> and Pingkai Ouyang<sup>a</sup>

#### Table of contents:

<b>Experimental Procedures</b> .....	3
Chemicals and Materials.....	3
Process of 2KGA Dehydration .....	3
Derivatisation of the intermediate .....	4
Acetylation of Me-2KGA .....	4
Computational details .....	4
Analytical Equipment .....	5
Fig. S1 HPLC detected results of 2KGA dehydration in DMSO .....	7
Detected UV absorption (254nm) in 2KGA dehydration liquid. ....	7
Retention time of side product and furfural at 254 nm.....	7
UV absorption spectrum of side product .....	7
UV absorption spectrum of furfural .....	8
UV absorption spectrum of UX .....	8
Fig. S2 HRMS of UX. ....	9
Fig. S3 <sup>13</sup> C NMR Spectra of UX. ....	10
Fig. S4 Comparison of HPLC retention times. ....	11
Fig. S5 Crystal Structure of UX. ....	12
Table. S1 Crystal data and structure refinement for KEAC. ....	12
Table. S2 Fractional Atomic Coordinates (×104) and Equivalent Isotropic Displacement Parameters (Å <sup>2</sup> ×103) for KEAC. ....	13
Table. S3 Anisotropic Displacement Parameters (Å <sup>2</sup> ×103) for KEAC <sup>a</sup> . ....	13
Table. S4 Bond Lengths for KEAC. ....	13
Table. S5 Bond Angles for KEAC. ....	14
Table. S6 Hydrogen Atom Coordinates (Å×104) and Isotropic Displacement Parameters (Å <sup>2</sup> ×103) for KEAC. ....	14
Fig. S6 GC detection of Me-2FGA and nBu-2FGA.....	15
Fig. S7. <sup>1</sup> H and <sup>13</sup> C NMR Spectra of Me-2FGA.....	16

Fig. S8. $^1\text{H}$ and $^{13}\text{C}$ NMR Spectra of nBu-2FGA. ....	17
Fig. S9 Appearance of five commercial solid catalysts. ....	18
Fig. S10 Effect of temperatures on the dehydration of 2KGA in n-butanol. ....	18
Table. S7 $^1\text{H}$ and $^{13}\text{C}$ NMR assignments for 2KGA and Me-2KGA <sup>a</sup> : ....	19
Fig. S11 $^1\text{H}$ and $^{13}\text{C}$ NMR Spectra of 2KGA in $\text{CD}_3\text{OD}$ . ....	20
Fig. S12 $^1\text{H}$ and $^{13}\text{C}$ NMR Spectra of Me-2KGA in $\text{CD}_3\text{OD}$ . ....	21
Fig. S13 $^1\text{H}$ and $^{13}\text{C}$ NMR Spectra of 2KGA in $(\text{CD}_3)_2\text{SO}$ . ....	22
Fig. S14 $^1\text{H}$ and $^{13}\text{C}$ NMR Spectra of 2KGA in $\text{D}_2\text{O}$ . ....	23
Fig. S15 HMBC Spectra of 2KGA in $\text{CD}_3\text{OD}$ . ....	24
Fig. S16 Potential energy surface (PES) for Dehydrogenation of IM3-Me. ....	25
Fig. S17 The key bond distances in angstroms Å. ....	26
Fig. S18 Potential energy surface (PES) for Dehydrogenation of IM2-H. ....	27
General Method of derivations ....	28
Fig. S19 Synthesis of $\lambda^5$ -Azaneyl(Z)-2-(furan-2-yl)-2-(methoxyimino)acetate. ....	28
Fig. S20 Aryl substitution. ....	28
Fig. S21 Decarboxylation coupling. ....	28
Fig. S22 Amidation. ....	29
Fig. S23 Amidation reduction. ....	29
Table. S9 Characterization of derivatives. ....	30
Fig. S24 $^1\text{H}$ and $^{13}\text{C}$ NMR Spectra of derivatives. ....	33
References. ....	40

<sup>a</sup> College of Biotechnology and Pharmaceutical Engineering, Nanjing Tech University, 30 South Puzhu Road, Nanjing, 211816 (P. R. China)

<sup>b</sup> Institute of Advanced Synthesis, School of Chemistry and molecular Engineering, Nanjing Tech University, 30 South Puzhu Road, Nanjing, 211816 (P. R. China).

<sup>c</sup> Suzhou Cornigs Polyols Co., Ltd. 1183 Wuzhong Avenue, Suzhou, 215000 (P. R. China)

\*Corresponding author Email: [csaofeiw@njtech.edu.cn](mailto:csaofeiw@njtech.edu.cn), [hlwu@njtech.edu.cn](mailto:hlwu@njtech.edu.cn), [ias\\_llzhao@njtech.edu.cn](mailto:ias_llzhao@njtech.edu.cn)

## Experimental Procedures

### Chemicals and Materials

The 2-keto-L-gluconic acid (2KGA, 95%) was purchased from Hengyou (Anhui, China), comanic acid (99%), coumalic acid (99%), methanol (AR), n-butanol (AR), N-methyl pyrrolidone (NMP, AR), methyl isobutyl ketone (MIBK, AR), acetonitrile (HPLC,  $\geq 99\%$ ), and sulfolane (AR) were purchased from Macklin (Shanghai, China). Dimethyl sulfoxide (DMSO, AR), acetone (AR), 2-butanone (AR), 2-Methyltetrahydrofuran (MTHF, AR), 1,4-dioxane (DIO, AR),  $\text{SOCl}_2$  (AR), anhydrous sodium sulfate (AR), and sodium chloride (AR) were purchased from Sinopharm (Shanghai, China). Dichloromethane (AR), petroleum ether (60-90°C,  $\geq 96\%$ ), N-hexane (HPLC,  $\geq 99\%$ ), ethyl acetate (AR,  $\geq 99\%$ ), N,N-dimethylacetamide (AR),  $\gamma$ -valerolactone (GVL, AR), (BMIm)BF<sub>4</sub> (AR), (BMIm)HSO<sub>4</sub> (AR), (EMIm)Cl (AR), (BMIm)Cl (AR), concentrated sulfuric acid (H<sub>2</sub>SO<sub>4</sub>, 98%), concentrated hydrochloric acid (HCl, 36%), phosphoric acid (H<sub>3</sub>PO<sub>4</sub>,  $\geq 99\%$ ), hydrobromic acid (HBr, 98%), trifluoroacetic acid (TFA, 99%), trifluoromethanesulfonic acid (TfOH, AR), methanesulfonic acid (MSA, AR), p-toluenesulfonic acid (p-TSA, AR), and anhydrous calcium hydride (AR) were purchased from Aladdin (Shanghai, China). Amberlyst 15, HND-590, HND-580, HND-12, HND-8, were purchased from Nanda Synthetic (Jiangsu, China).

### Process of 2KGA Dehydration

The following process was used for the experiments reported in Table 1: Pressure tube (15 mL) were equipped with magnetic stirring. The tube was charged with a solvent (5 mL) and H<sub>2</sub>SO<sub>4</sub> (9 mmol). The substrate 2KGA (500 mg) dissolved rapidly in the solutions. The reaction mixtures were heated to 100 °C for 3 hours. After the reaction, the red-brown solution was cooled to room temperature, and concentrated at 40 °C under vacuum using a rotary evaporator. The products were separated by silica gel column chromatography (petroleum ether/ethyl acetate 9:1 and 10:1) to give the pure compounds as slightly yellow crystalline solids (product of alcohol solvents), and as purple-black crystalline solids (product of DMSO system). The products were analysed by <sup>1</sup>H/<sup>13</sup>C NMR spectroscopy, HPLC, GC, HRMS, and X-ray single crystal diffraction.

2FGA (MW: 140): <sup>13</sup>C NMR (75 MHz, CDCl<sub>3</sub>):  $\delta$  170.10 (s), 159.88 (s), 150.66 (s), 148.54 (s), 127.80 (s), 113.44 (s). <sup>1</sup>H NMR (400 MHz, CDCl<sub>3</sub>):  $\delta$  8.58 (s, 1H), 8.07 (s, 1H), 7.82 (s, 1H), 6.67 (s, 1H).

Me-2FGA (MW: 154): <sup>13</sup>C NMR (75 MHz, CDCl<sub>3</sub>):  $\delta$  170.40 (s), 161.11 (s), 149.42 (s), 124.64 (s), 112.80 (s), 52.87 (s). <sup>1</sup>H NMR (400 MHz, CDCl<sub>3</sub>):  $\delta$  7.73 (d, J = 12.1 Hz, 4H), 6.61 (s, 2H), 3.94 (s, 7H).

nBu-2FGA (MW: 196): <sup>13</sup>C NMR (75 MHz, CDCl<sub>3</sub>):  $\delta$  171.33 (s), 161.31 (s), 149.89 (s), 149.66 (d, J = 26.5 Hz), 124.36 (s), 112.98 (s), 66.37 (s), 30.38 (s), 18.98 (s), 13.51 (s). <sup>1</sup>H NMR (400 MHz, CDCl<sub>3</sub>):  $\delta$  7.69 (d, J = 0.9 Hz, 1H), 7.58 (d, J = 3.6 Hz, 1H),

6.54 (d, J = 2.0 Hz, 1H), 4.25 (s, 2H), 1.66 (s, 2H), 1.34 (d, J = 7.6 Hz, 2H), 0.85 (s, 3H).

The yields of 2FGA, Me-2FGA, and nBu-2FGA were defined by Equation (1).

$$\text{Yield [mol\%]} = \frac{\text{moles of product detected}}{\text{moles of inputted substrate}} \times 100\% \quad (1)$$

The isolated yield of Me-2FGA was defined by Equation (2).

$$\text{Yield [mol\%]} = \frac{\text{quality of isolated Me - 2FGA} / M_{\text{Me - 2FGA}}}{\text{moles of inputted Me - 2KGA}} \times 100\% \quad (2)$$

### Derivatisation of the intermediate

High-temperature high-pressure reactor (100 mL) was equipped with a magnetic stirring bar under nitrogen atmosphere (1 MPa). The reactor was charged with methanol (50 mL) and H<sub>2</sub>SO<sub>4</sub> (63 mmol). The substrate Me-2KGA (3.75 g) dissolved in the solutions. The reaction mixtures were heated to 110 °C for 15 mins, and immediately cooled to room temperature. Then the brown mix was added with sodium bicarbonate solution until the pH value was neutral, and separated the precipitation of sodium sulfate. After decolorisation, a clear and slightly yellow solution was obtained and concentrated at 40 °C under vacuum using a rotary evaporator to gain the intermediate. Subsequently, the intermediate (300 mg) was dissolved in the dichloromethane (9 mL), added 2.4 mmol acetic anhydride and 4 mmol pyridine step by step, and stirred at room temperature for 3.5 hours. Then the right amount of water was added, and the water layer was extracted with ethyl acetate. The organic layer was washed twice by 2 M HCl and water, respectively, dried over anhydrous sodium sulfate, and concentrated at 40 °C to gain the crude products. The crude products were separated by silica gel column chromatography (petroleum ether/ethyl acetate 4:1) to achieve the mixture of acetylation. The acetylated intermediate was analysed by <sup>1</sup>H/<sup>13</sup>C NMR spectroscopy, HRMS, and two-dimensional NMR spectroscopy DOSY.

### Acetylation of Me-2KGA

To Me-2KGA (1 mmol) in dichloromethane (9 mL) was added sequentially acetic anhydride (partial: 4 mmol; complete: 8 mmol), and pyridine (partial: 4 mmol; complete: 8 mmol). The reaction mixture was stirred at RT for 2.5 h and quenched by dilution with water. The aqueous phase was extracted with ethyl acetate and the organic phase was washed two times with 1 N HCl and water. The organic phase was dried over MgSO<sub>4</sub> and evaporated under reduced pressure. The acetylated 2KGA methyl ester was obtained as a primrose liquid.

### Computational details

Geometry optimizations without symmetry restriction were carried out with the Gaussian 16 program.<sup>1</sup> Specifically, geometry optimizations were firstly performed at the B3LYP<sup>2</sup>/def2-SVP<sup>3-5</sup> level with Grimme's GD3BJ dispersion corrections.<sup>6</sup> The

solvation effects of the experimentally used solvent (i.e., Methanol) were taken into consideration by using the Cramer–Truhlar continuum solvation model SMD.<sup>7</sup> Vibrational frequency calculations at the same level were performed for all stationary points to identify whether they were local minima (no imaginary frequencies) or transition structures (only one imaginary frequency), and to derive the thermochemical corrections for the enthalpies and free energies. Intrinsic reaction coordinate (IRC)<sup>8</sup> calculations were conducted to verify the critical reaction steps involved in our proposed mechanisms. The energetic results were then improved by the single-point calculations at the B3LYP+D3(BJ)/6-311+G(d,p) level<sup>9</sup> with the solvation effects included. Unless otherwise stated, the B3LYP+D3(BJ)/6-311+G(d,p) (smd, solvent = Methanol)/B3LYP +D3(BJ)/def2-SVP (smd, solvent = Methanol) Gibbs free energies (in kcal mol<sup>-1</sup>) are used in the following discussion, while the electronic energies are also given in the related figures for reference.

### **Analytical Equipment**

**TLC** was performed using Silica gel HSGF254 plates (160 Glass plates, 2.5 x 7.5 cm, Jiangyou). Major products of dehydration were analysed using the following procedure. 2FGA, Mobile phase: dichloromethane/methanol (10:1). Me-2FGA and nBu-2FGA, Mobile phase: petroleum ether/ethyl acetate (9:1). TLC plates were developed and dried, and the products were detected under UV light (254 nm).

**HPLC** analyses were performed using Shimadzu LC-20A with a UV detector. The 2FGA and FF were separated on a Bio-Rad HPLC column (Aminex HPX-87H, 300 x 7.8 mm) under 284 nm and 275 nm, respectively. 0.5 mM H<sub>2</sub>SO<sub>4</sub> was used as the mobile phase with a flow of 0.6 mLmin<sup>-1</sup>. Program: hold 60 min at 35 °C. The retention times of 2FGA and FF were 10.536 and 54.623 mins, respectively. The 2KGA was separated on an Elite HPLC column (C18, 300 x 7.8 mm) under 210 nm. Mobile phase: a mixture of ethyl acetate 0.5 mM H<sub>2</sub>SO<sub>4</sub>/acetonitrile (9:1). Program: hold 60 min at 40 °C with a flow of 1 mLmin<sup>-1</sup>. The retention times of 2KGA was 2.795 mins

**GC** analyses were performed using Shimadzu GC-2010 Plus with a hydrogen flame ionisation detector. Products were separated on a Shimadzu GC column (Rtx-VMS 30 m x 0.25 mm x 1.4 µm). Helium was used as the carrier gas with a flow of 1 mLmin<sup>-1</sup>. Temperature program: hold 5 min at 40 °C, ramp 7.5 °Cmin<sup>-1</sup>, final temperature 240 °C and hold 15 min. The retention times of M2FGA and nBu-2FGA were 27.989 and 32.414 mins, respectively.

**NMR** spectra were recorded on a Bruker Av400III HD operating at 400.13 MHz (<sup>1</sup>H) and 75.62 MHz (<sup>13</sup>C) in CDCl<sub>3</sub> ((99.9 at% D, Aldrich) MeOD-D<sub>4</sub> (≥99.8 at% D, containing 0.03% v/v TMS, Aldrich) or D<sub>2</sub>O (99.9 at% D, Aldrich). D<sub>2</sub>O solutions were adjusted to the desired pH value with D<sub>2</sub>SO<sub>4</sub> (35 wt% solution in D<sub>2</sub>O, 99 atom % D, Aldrich). Chemical shifts are quoted in parts per million (ppm) referenced to the appropriate solvent peaks or 0 ppm for TMS.

**HMBC** experiments were performed with the Bruker standard 1H detected heteronuclear multiple bond correlation etgpl3nd pulse sequence.

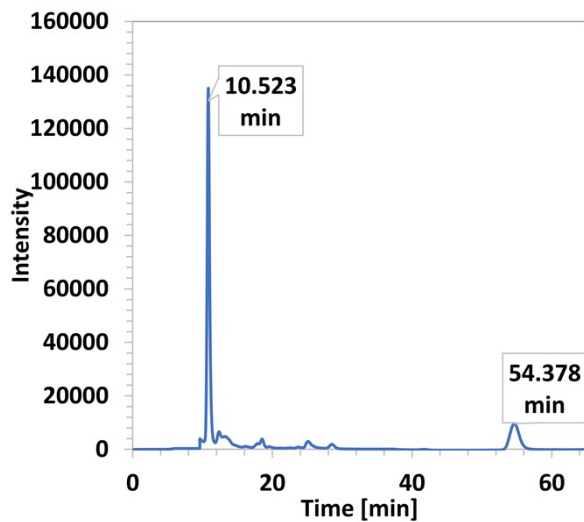
**DOSY** experiments were performed with the Bruker standard ledbpgp2s pulse sequence. For each DOSY-NMR experiment, 32 spectra with 32K data points were collected. The diffusion time ( $\Delta$ ) was 200 ms. The duration of the pulse field gradient ( $\delta/2$ ) was 550  $\mu$ s. The delay for gradient recovery was 100  $\mu$ s and the eddy current delay was 5 ms. The additional spoiling gradients was 800  $\mu$ s. All the measurements were performed at 298 K without sample spinning.

**HRMS** spectra was used a Thermo QE-HFX mass selective detector (ESI, mass range 50–6000 Dalton, 200 ms sample speed), and carried out in negative ion mode for detection.

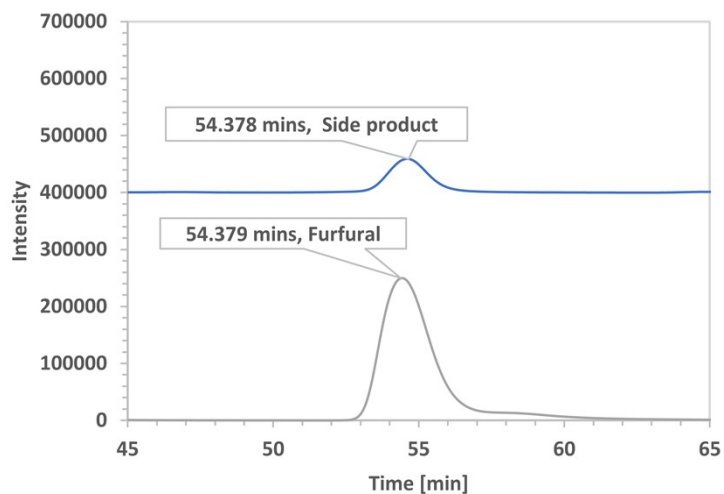
**X-ray single crystal diffraction** was performed using Bruker D8 VENTURE. The crystals were grown by means of evaporation of a mixture of ethyl acetate/n-hexane (1:1) at room temperature. A suitable crystal was selected and put on a 'D8 VENTURE' diffractometer. The crystal was kept at 170.0 K during data collection. Using Olex2,<sup>10</sup> the structure was solved with the ShelXT structure solution program using Intrinsic Phasing and refined with the ShelXL refinement package using Least Squares minimisation.<sup>11</sup>

**Fig. S1 HPLC detected results of 2KGA dehydration in DMSO**

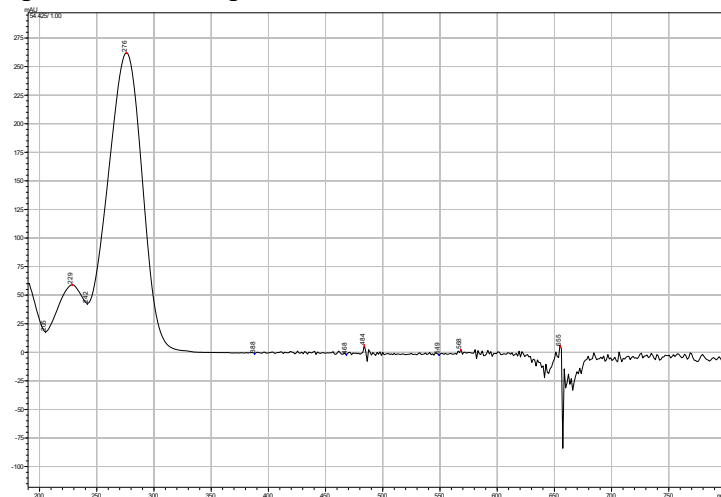
Detected UV absorption (254nm) in 2KGA dehydration liquid.



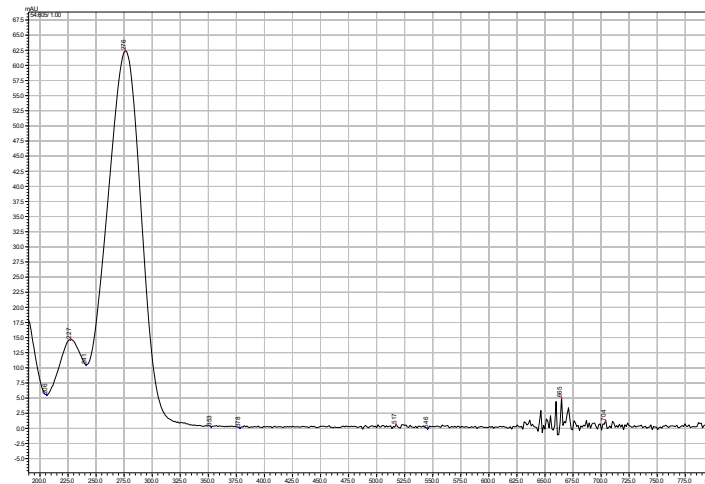
Retention time of side product and furfural at 254 nm.



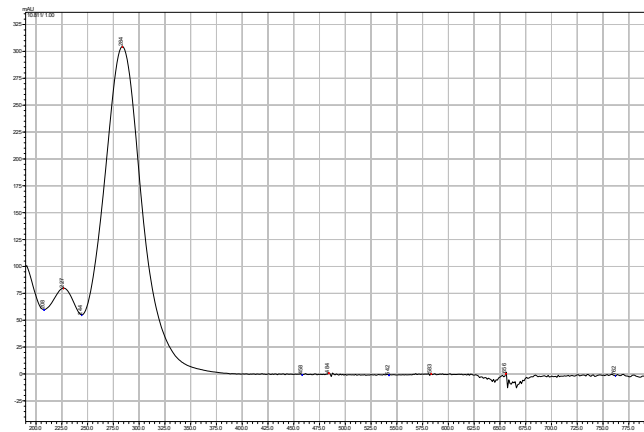
UV absorption spectrum of side product



## UV absorption spectrum of furfural



## UV absorption spectrum of UX



★ HPLC condition: HPX-87H column under 5 mM H<sub>2</sub>SO<sub>4</sub> 0.6 mL min<sup>-1</sup>.



**Fig. S2 HRMS of UX.**

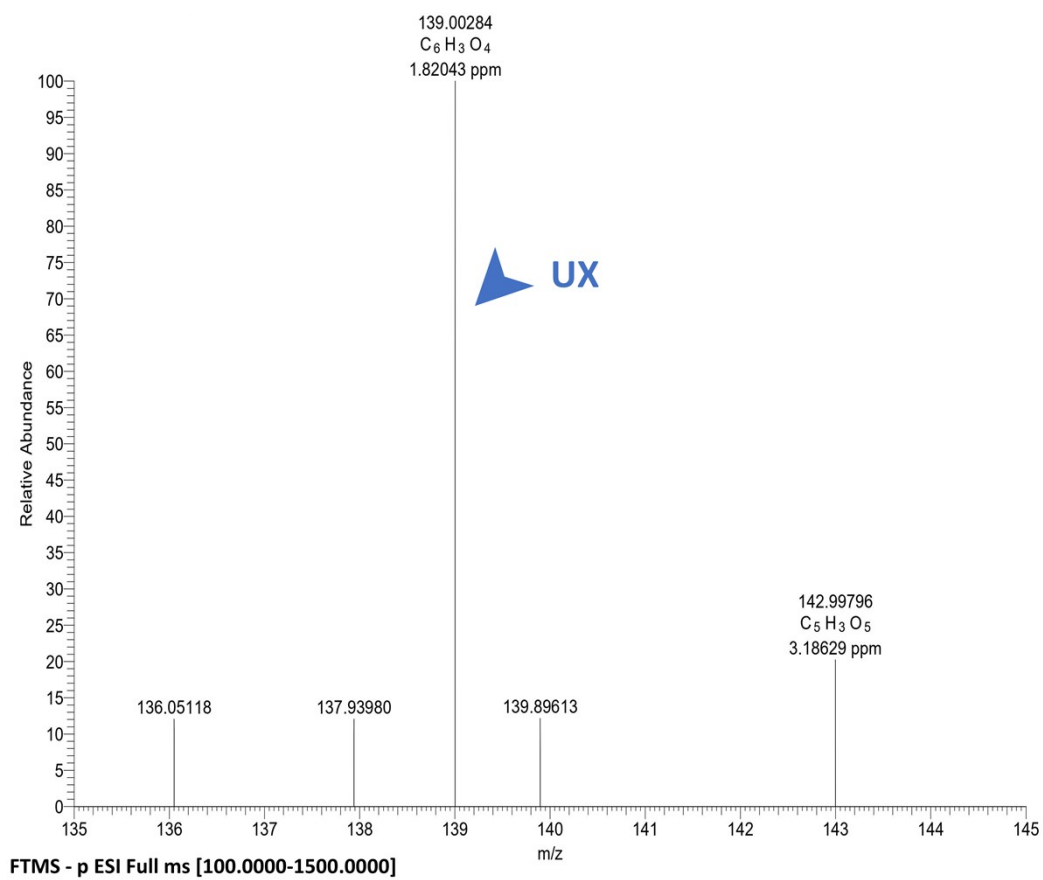


Fig. S3  $^{13}\text{C}$  NMR Spectra of UX.

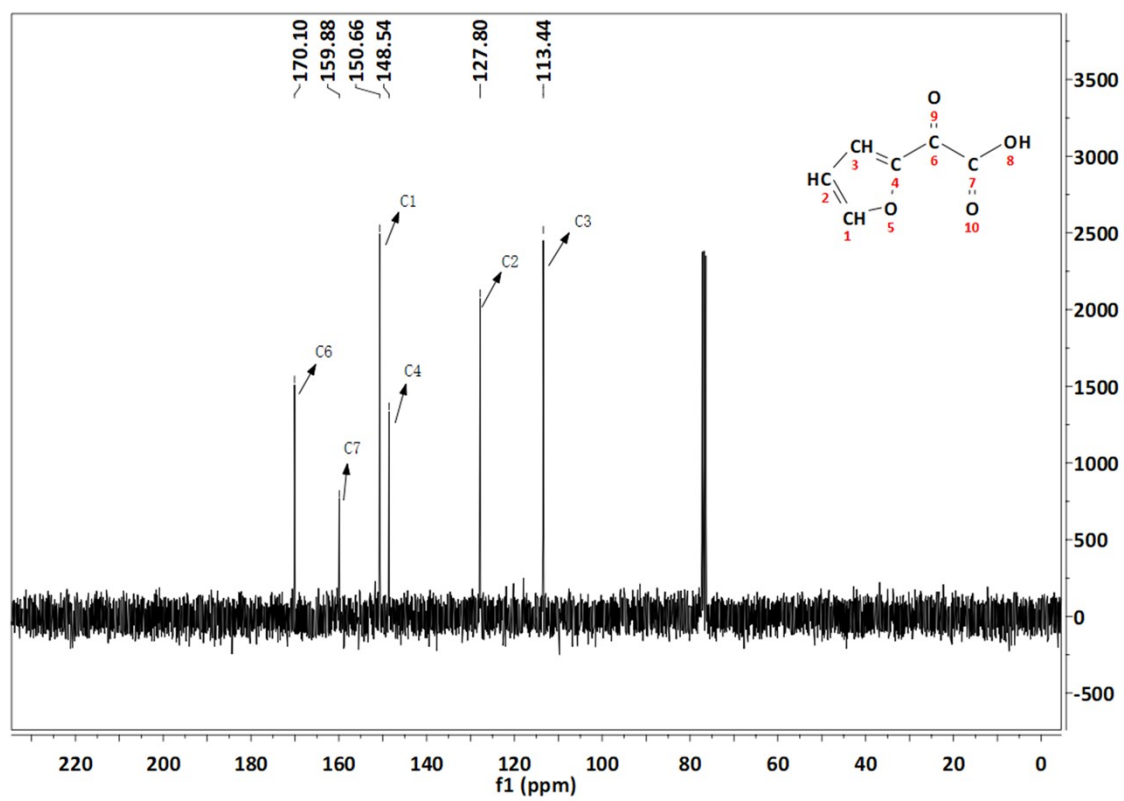
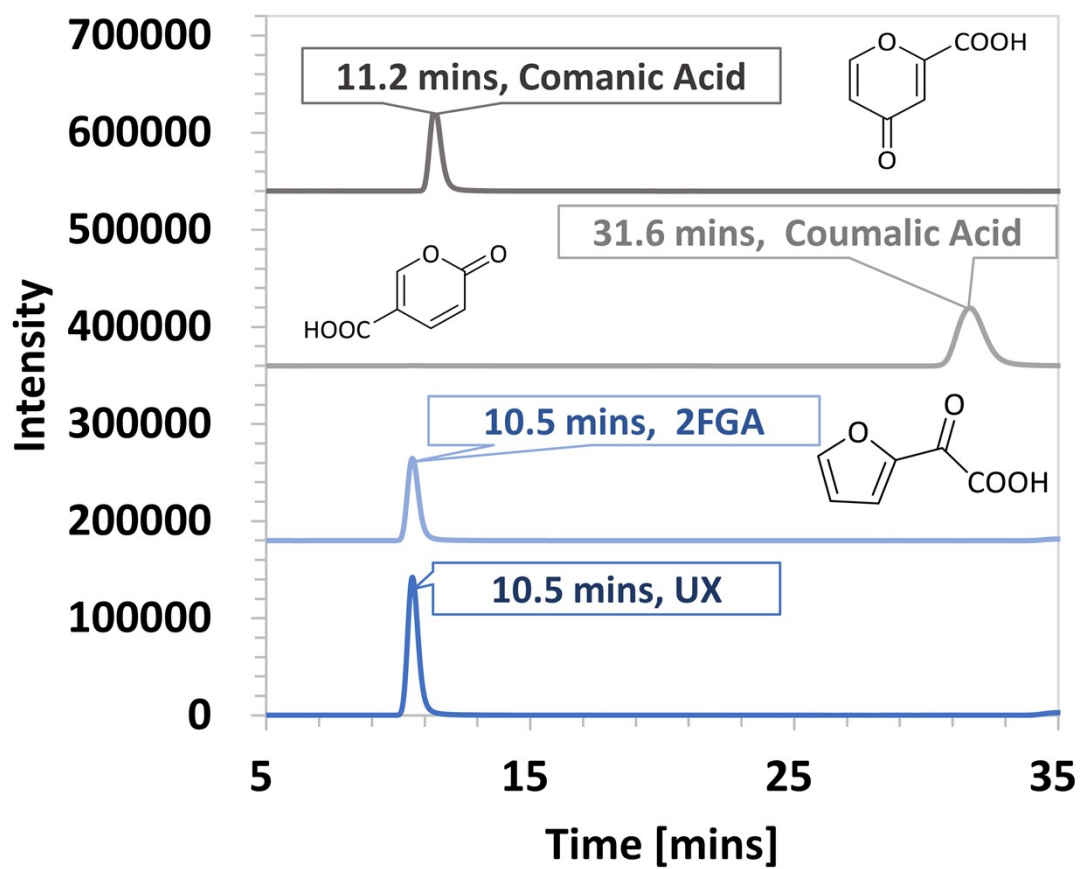
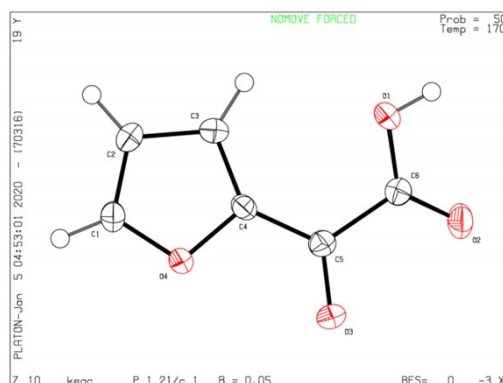


Fig. S4 Comparison of HPLC retention times.



**Fig. S5 Crystal Structure of UX.**



Crystal structure determination. Crystal Data for C<sub>6</sub>H<sub>4</sub>O<sub>4</sub> (M = 140.09 g/mol): monoclinic, space group P2<sub>1</sub>/c (no. 14), a = 7.7533(4) Å, b = 9.7624(6) Å, c = 7.4178(4) Å, β = 93.892(2)°, V = 560.16(5) Å<sup>3</sup>, Z = 4, T = 170.0 K, μ(MoKα) = 0.144 mm<sup>-1</sup>, D<sub>calc</sub> = 1.661 g/cm<sup>3</sup>, 5252 reflections measured (5.266° ≤ 2θ ≤ 52.896°), 1142 unique (R<sub>int</sub> = 0.0442, R<sub>sigma</sub> = 0.0390) which were used in all calculations. The final R<sub>1</sub> was 0.0481 (I > 2σ(I)) and wR<sub>2</sub> was 0.1044 (all data)

**Table. S1 Crystal data and structure refinement for KEAC.**

Empirical formula	C <sub>4</sub> H <sub>6</sub> O <sub>4</sub>
Formula weight	140.09
Temperature / K	170
Crystal system	monoclinic
Space group	P2 <sub>1</sub> /c
a/Å	7.7533(4)
b/Å	9.7624(6)
c/Å	7.4178(4)
α/°	90
β/°	93.892(2)
γ/°	90
Volume/Å <sup>3</sup>	560.16(5)
Z	4
ρ <sub>cal</sub> cg / cm <sup>3</sup>	1.661
μ / mm <sup>-1</sup>	0.144
F (000)	288.0
Crystal size / mm <sup>3</sup>	0.16 × 0.12 × 0.08
Radiation	MoKα (λ = 0.71073)
2θ range for data collection/°	5.266 to 52.896
Index ranges	-8 ≤ h ≤ 9, -12 ≤ k ≤ 12, -8 ≤ l ≤ 9
Reflections collected	5252
Independent reflections	1142 [R <sub>int</sub> = 0.0442, R <sub>sigma</sub> = 0.0390]
Data/restraints/parameters	1142/0/92
Goodness-of-fit on F <sup>2</sup>	1.129
Final R indexes [I >= 2σ(I)]	R <sub>1</sub> = 0.0481, wR <sub>2</sub> = 0.0935
Final R indexes [all data]	R <sub>1</sub> = 0.0681, wR <sub>2</sub> = 0.1044
Largest diff. peak/hole / e Å <sup>-3</sup>	0.24/-0.25

**Table. S2 Fractional Atomic Coordinates ( $\times 10^4$ ) and Equivalent Isotropic Displacement Parameters ( $\text{\AA}^2 \times 10^3$ ) for KEAC.**

Atom	x	y	z	U(eq) <sup>a</sup>
O4	5271.3(19)	6262.3(15)	4168(2)	25.4(4)
O1	8899(2)	9254.6(15)	2948(2)	31.6(4)
O3	8390(2)	5725.3(15)	3044(2)	31.7(4)
O2	10326(2)	7650.9(17)	1465(2)	34.0(5)
C4	6276(3)	7328(2)	3619(3)	20.7(5)
C3	5374(3)	8529(2)	3719(3)	23.5(5)
C5	7932(3)	6927(2)	3048(3)	22.2(5)
C6	9195(3)	7998(2)	2387(3)	23.4(5)
C2	3761(3)	8192(2)	4368(3)	25.4(5)
C1	3766(3)	6821(2)	4617(3)	25.4(5)

<sup>a</sup> U<sub>eq</sub> is defined as 1/3 of the trace of the orthogonalised U<sub>ij</sub> tensor.

**Table. S3 Anisotropic Displacement Parameters ( $\text{\AA}^2 \times 10^3$ ) for KEAC <sup>a</sup>.**

Atom	U <sub>11</sub>	U <sub>22</sub>	U <sub>33</sub>	U <sub>23</sub>	U <sub>13</sub>	U <sub>12</sub>
O4	23.6(8)	18.0 (8)	36.1(10)	0.5(6)	12.2(7)	-1.7(6)
O1	28.8(9)	19.6 (8)	48.2(11)	1.7(7)	16.2(8)	-4.4(7)
O3	30.7(9)	18.1 (8)	48.0(11)	-2.17	15.2(8)	3.1(7)
O2	27.0(9)	34.6(10)	42.3(11)	-7.2(8)	16.2(8)	-6.1(7)
C4	22.2(11)	17.3(10)	23.0(12)	-0.2(8?)	4.0(9)	-3.9(9)
C3	25.7(11)	17.7(10)	27.4(12)	1.1(9)	3.1(9)	1.0(9)
C5	23.9(11)	20.1(11)	23.1(12)	-1.3(9)	4.4(9)	0.6(9)
C6	20.4(11)	22.3(11)	27.7(12)	1.4(9)	2.8(9)	0.6(9)
C2	20.8(11)	25.8(12)	30.1(13)	-0.3(10)	5.0(10)	4.3(9)
C1	20.2(11)	26.4(12)	30.4(13)	-1.5(10)	7.5(9)	-2.1(9)

<sup>a</sup> The Anisotropic displacement factor exponent takes the form:  $-2\pi^2 [h^2 a^2 U_{11} + 2hka \cdot b \cdot U_{12} + \dots]$ .

**Table. S4 Bond Lengths for KEAC.**

Atom	Atom	Length / $\text{\AA}$
O4	C4	1.377(2)
O4	C1	1.351(3)
O1	C6	1.321(3)
O3	C5	1.226(3)
O2	C6	1.197(3)
C4	C3	1.370(3)
C4	C5	1.433(3)
C3	C2	1.410(3)
C5	C6	1.536(3)
C2	C1	1.351(3)

**Table. S5 Bond Angles for KEAC.**

Atom	Aom	Atom	Angle / °
C1	O4	C4	106.47 ( 16 )
O4	C4	C5	114.63 ( 18 )
C3	C4	O4	109.25 ( 18 )
C3	C4	C5	136.1 ( 2 )
C4	C3	C2	106.62 ( 19 )
O3	C5	C4	121.88 ( 19 )
O3	C5	C6	117.34 ( 19 )
C4	C5	C6	120.77 ( 18 )
O1	C6	C5	113.85 ( 18 )
O2	C6	O1	126.3 ( 2 )
O2	C6	C5	119.8 ( 2 )
C1	C2	C3	106.50 ( 19 )
O4	C1	C2	111.15 ( 19 )

**Table. S6 Hydrogen Atom Coordinates ( $\text{\AA}\times 10^4$ ) and Isotropic Displacement Parameters ( $\text{\AA}^2\times 10^3$ ) for KEAC.**

Atom	x	y	z	U(eq)
H1	9675.09	9780.63	2617.45	47
H3	5760.96	9417.11	3410.41	28
H2	2849.51	8807.34	4587.58	30
H1A	2831.71	6315.88	5050.52	31

**Fig. S6 GC detection of Me-2FGA and nBu-2FGA.**

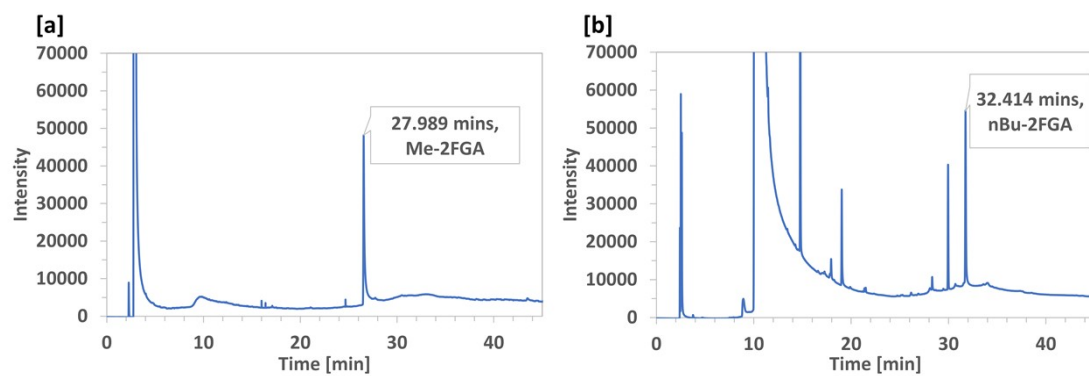


Fig. S7. <sup>1</sup>H and <sup>13</sup>C NMR Spectra of Me-2FGA.

Me-2FGA

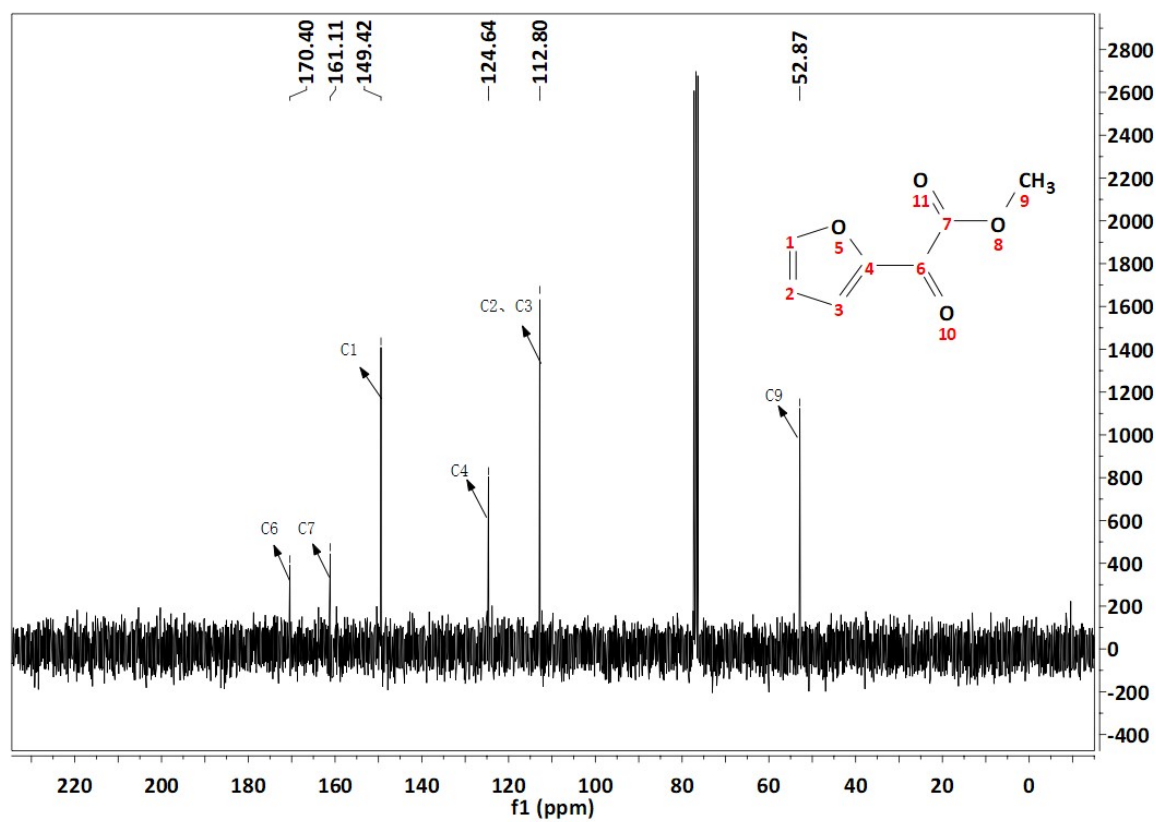
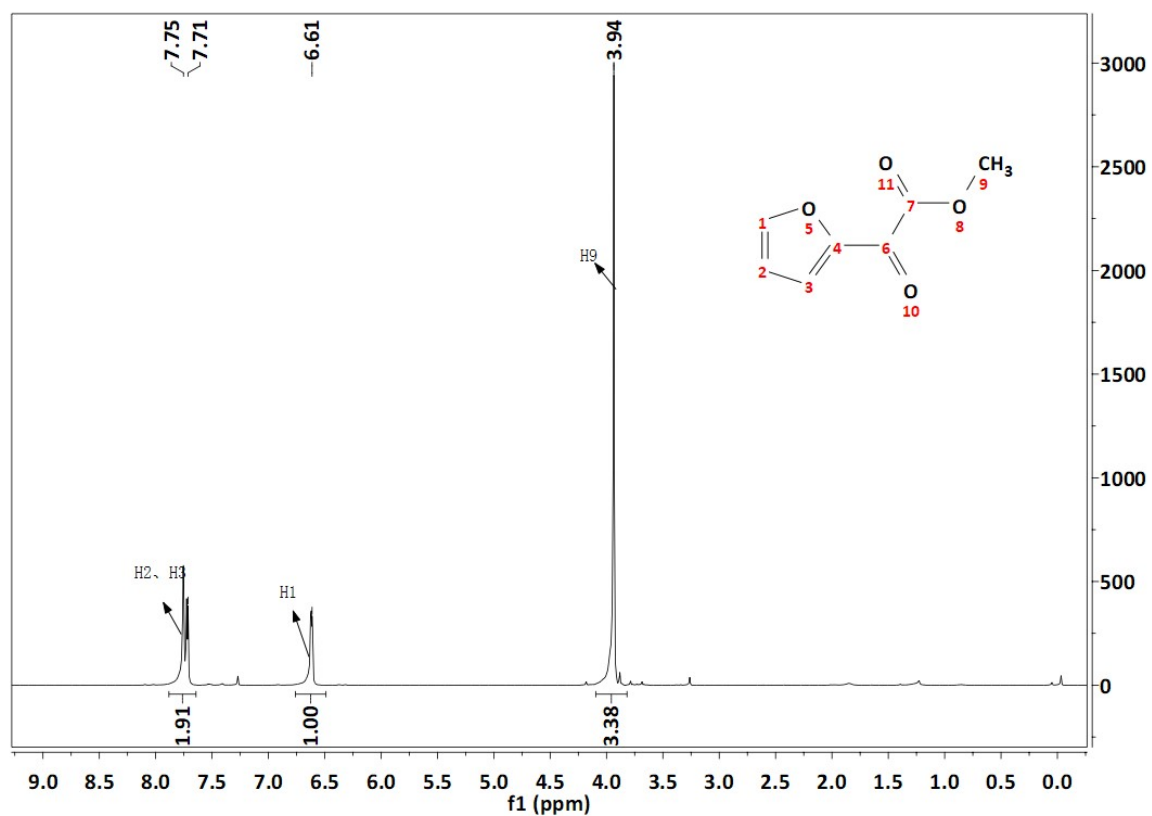
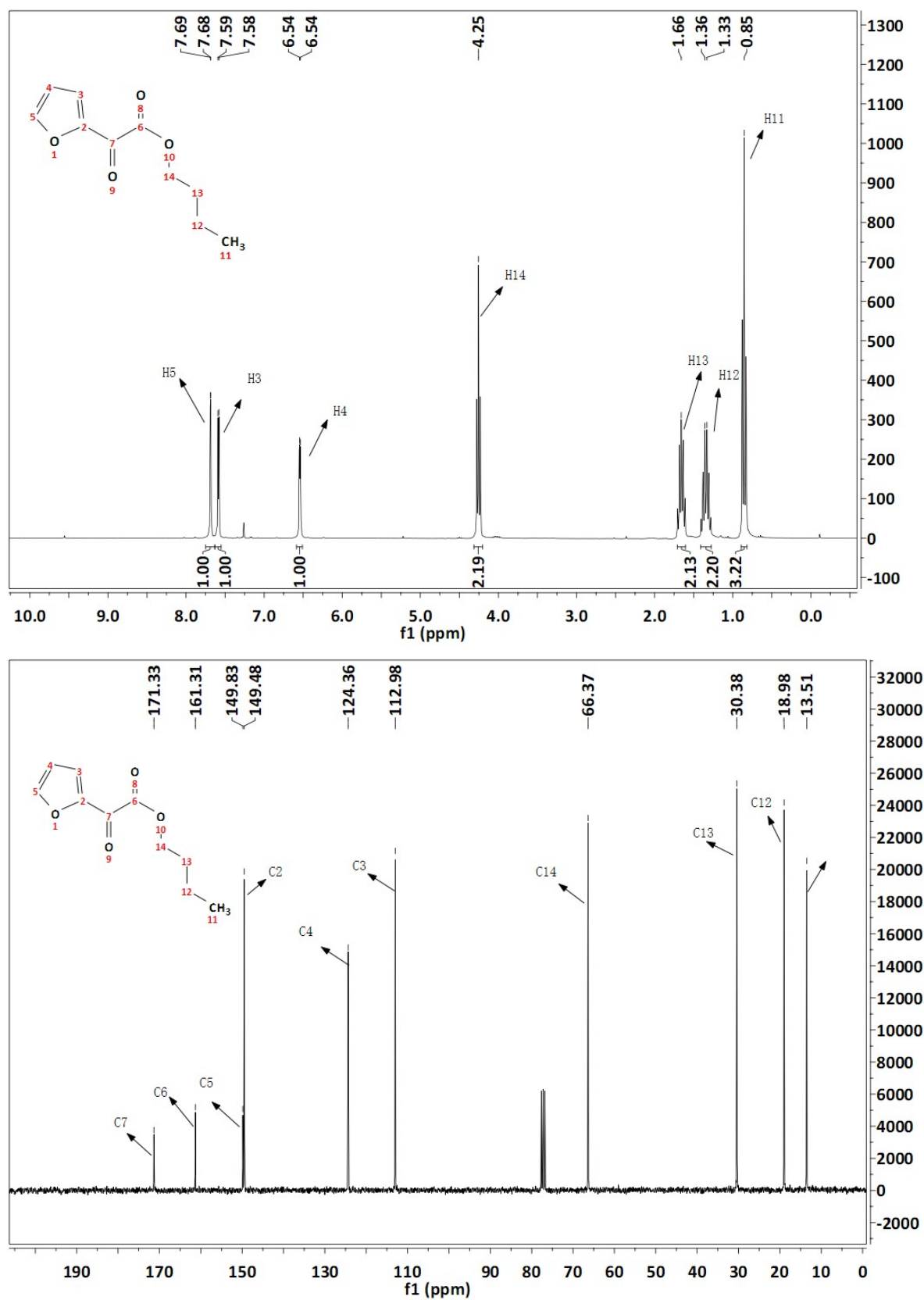




Fig. S8. <sup>1</sup>H and <sup>13</sup>C NMR Spectra of nBu-2FGA.

nBu-2FGA



**Fig. S9 Appearance of five commercial solid catalysts.**

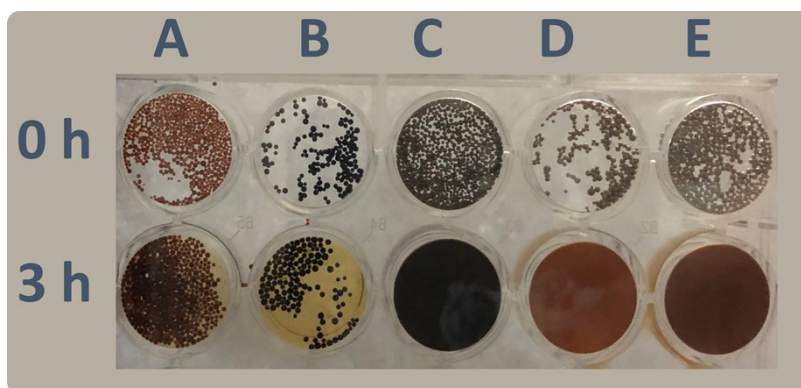
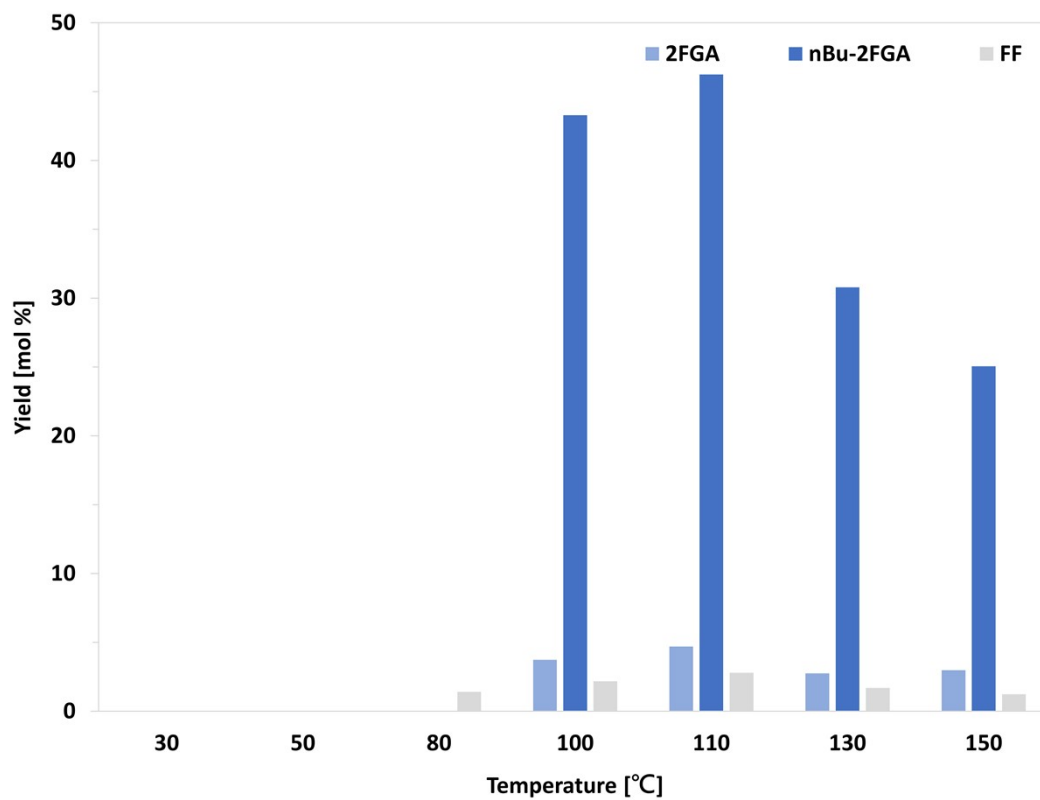


Fig. S9 Appearance of five commercial solid acid catalysts. Reaction condition: 2KGA 0.5g, n-butanol 5mL, catalyst 10 wt%, under 110°C for 3 hours. A: amberlyst-70; B: HND-590; C: HND-580; D: HND-12; E: HND-8.

**Fig. S10 Effect of temperatures on the dehydration of 2KGA in n-butanol.**



**Table. S7  $^1\text{H}$  and  $^{13}\text{C}$  NMR assignments for 2KGA and Me-2KGA <sup>a</sup>:**

	Me-2KGA		2KGA		
	$\delta_{\text{H}}$	$\delta_{\text{C}}$	$\delta_{\text{H}}$	$\delta_{\text{C}}$	HMBC
C-1	/	171.35	/	173.64	H-3, H-4, H-5
C-2	/	97.71	/	97.33	H-3, H-4, H-5, H-6
C-3	3.57	75.57	3.58	75.67	H-4, H-5, H-6
C-4	3.60	74.32	3.61	74.20	H-3, H-5, H-6
C-5	3.66	71.30	3.68	71.23	H-3, H-4, H-6
C-6	3.64, 3.69	64.20	3.66, 3.71	64.13	H-3, H-4, H-5

<sup>a</sup>: Conditions:  $^{13}\text{C}$  NMR: 75 MHz,  $\text{CD}_3\text{OD}$ ;  $^1\text{H}$  NMR: 300 MHz,  $\text{CD}_3\text{OD}$ .

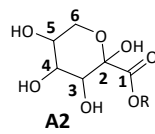
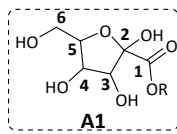
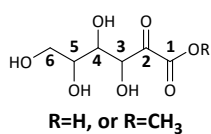


Fig. S11  $^1\text{H}$  and  $^{13}\text{C}$  NMR Spectra of 2KGA in  $\text{CD}_3\text{OD}$ .

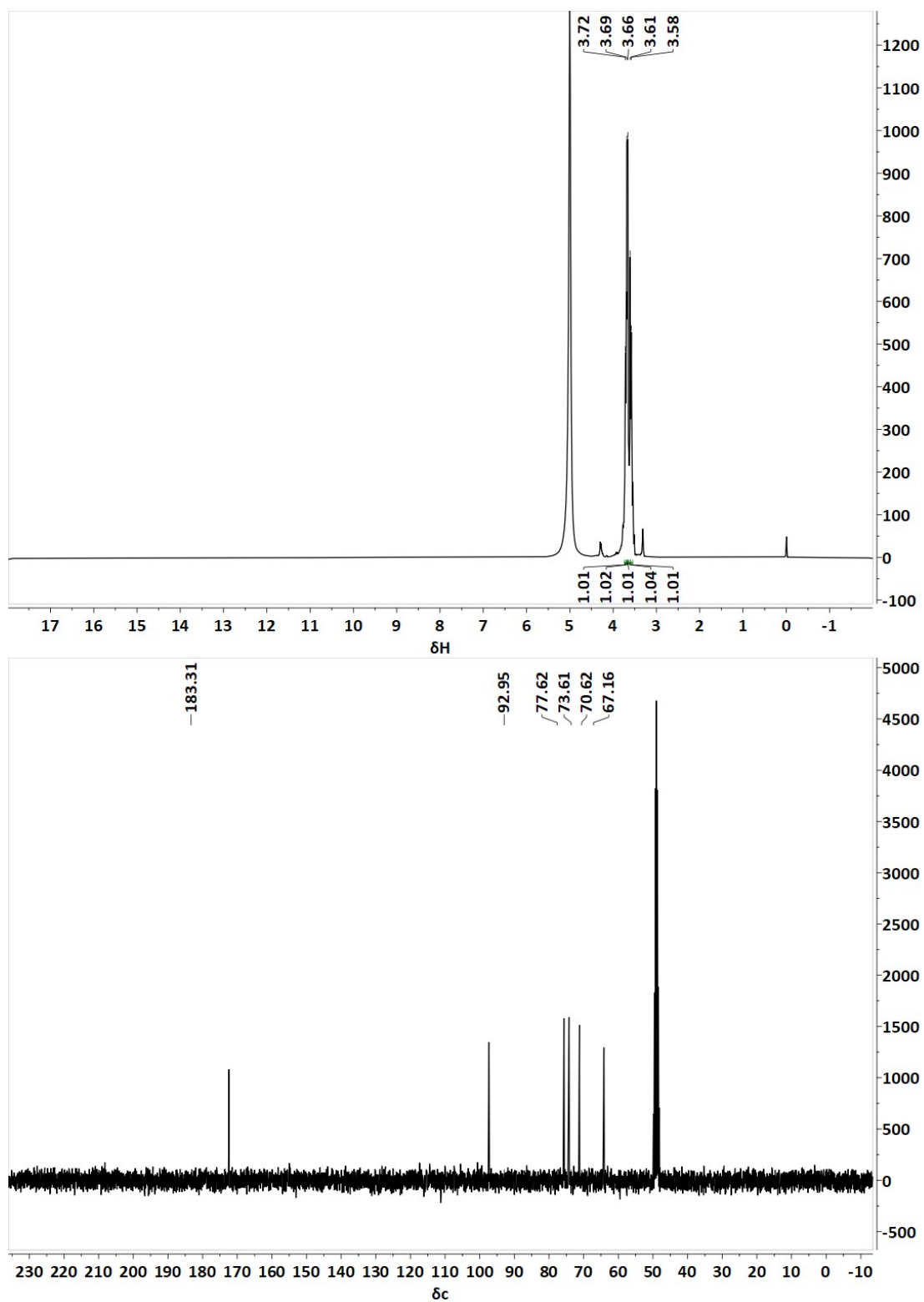


Fig. S12  $^1\text{H}$  and  $^{13}\text{C}$  NMR Spectra of Me-2KGA in  $\text{CD}_3\text{OD}$ .

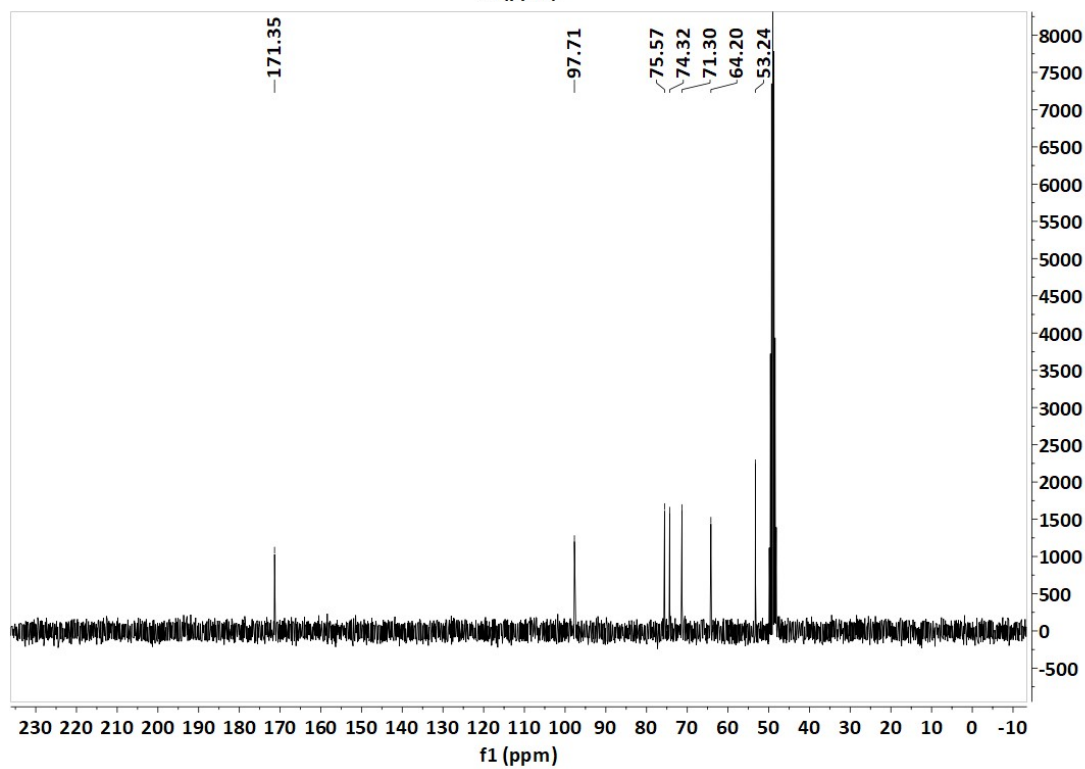
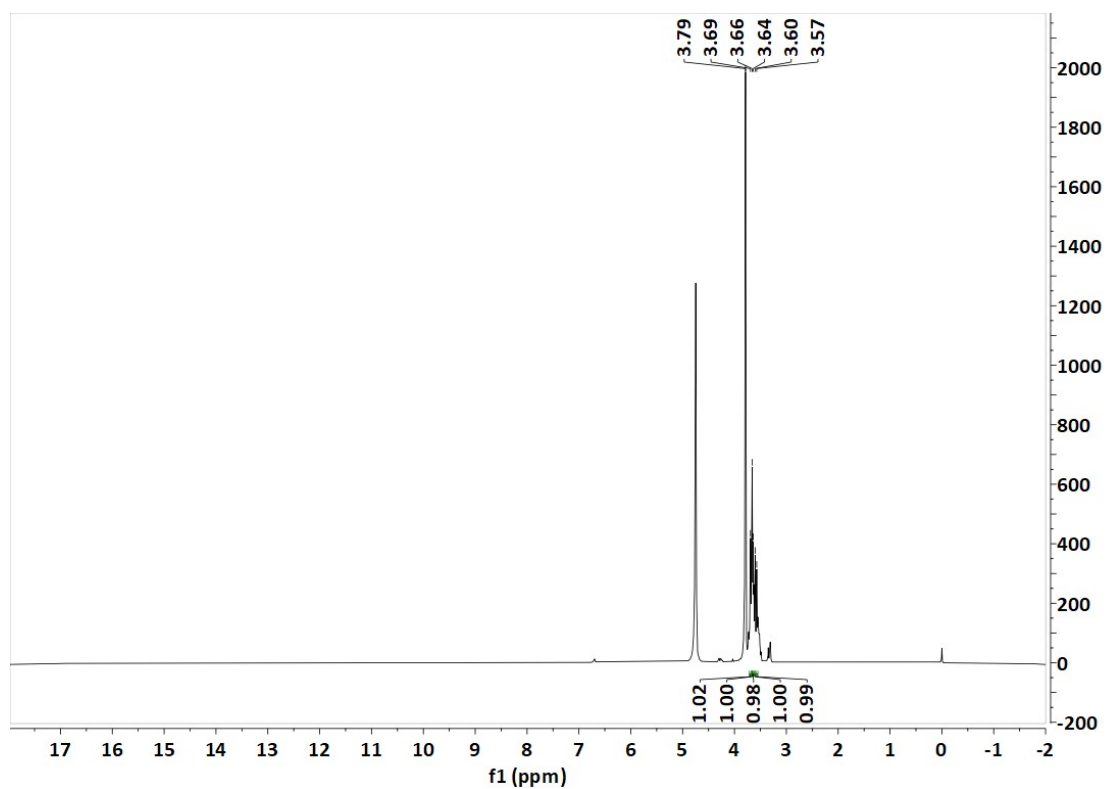


Fig. S13  $^1\text{H}$  and  $^{13}\text{C}$  NMR Spectra of 2KGA in  $(\text{CD}_3)_2\text{SO}$ .

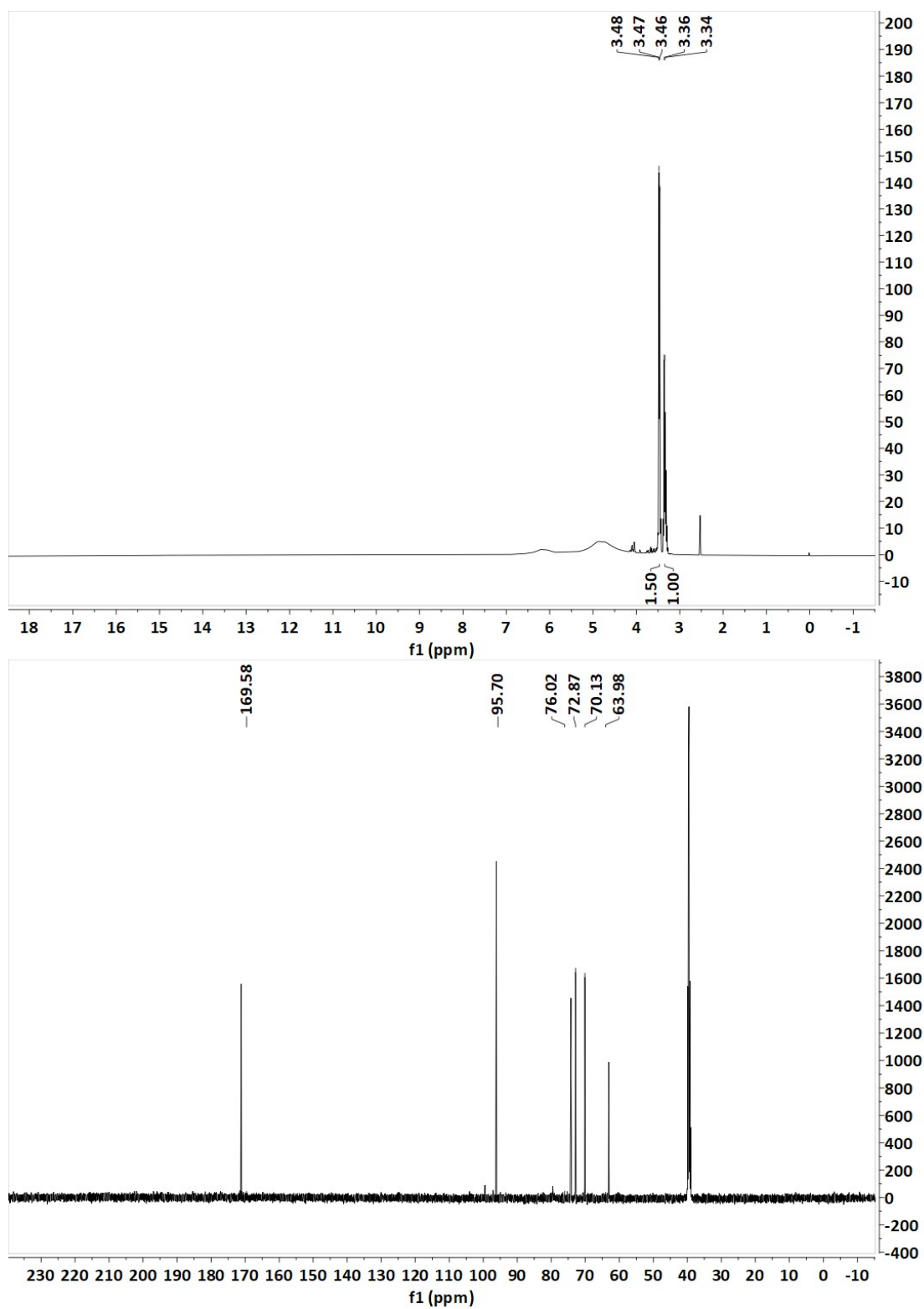


Fig. S14  $^1\text{H}$  and  $^{13}\text{C}$  NMR Spectra of 2KGA in  $\text{D}_2\text{O}$ .

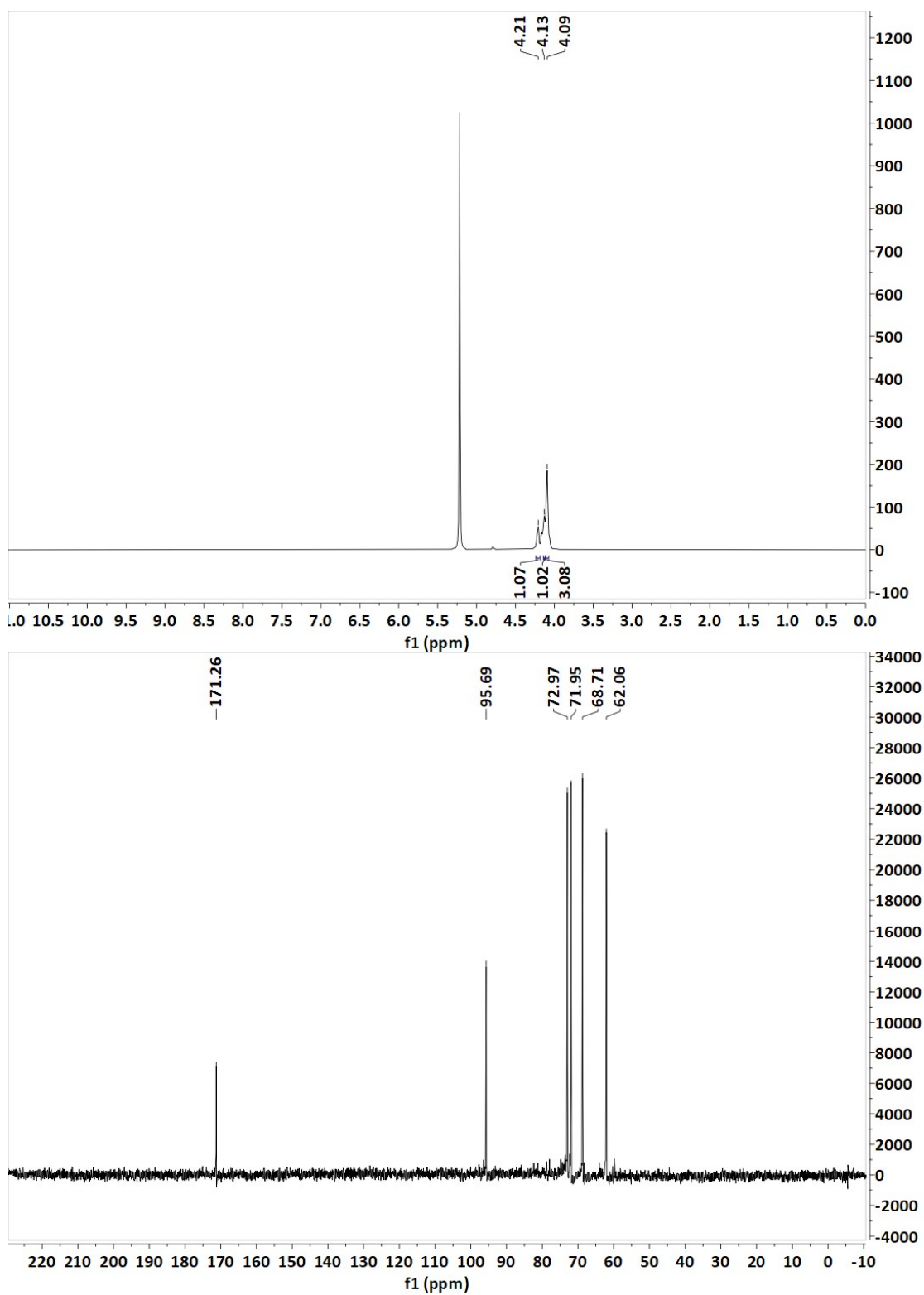


Fig. S15 HMBC Spectra of 2KGA in CD<sub>3</sub>OD.

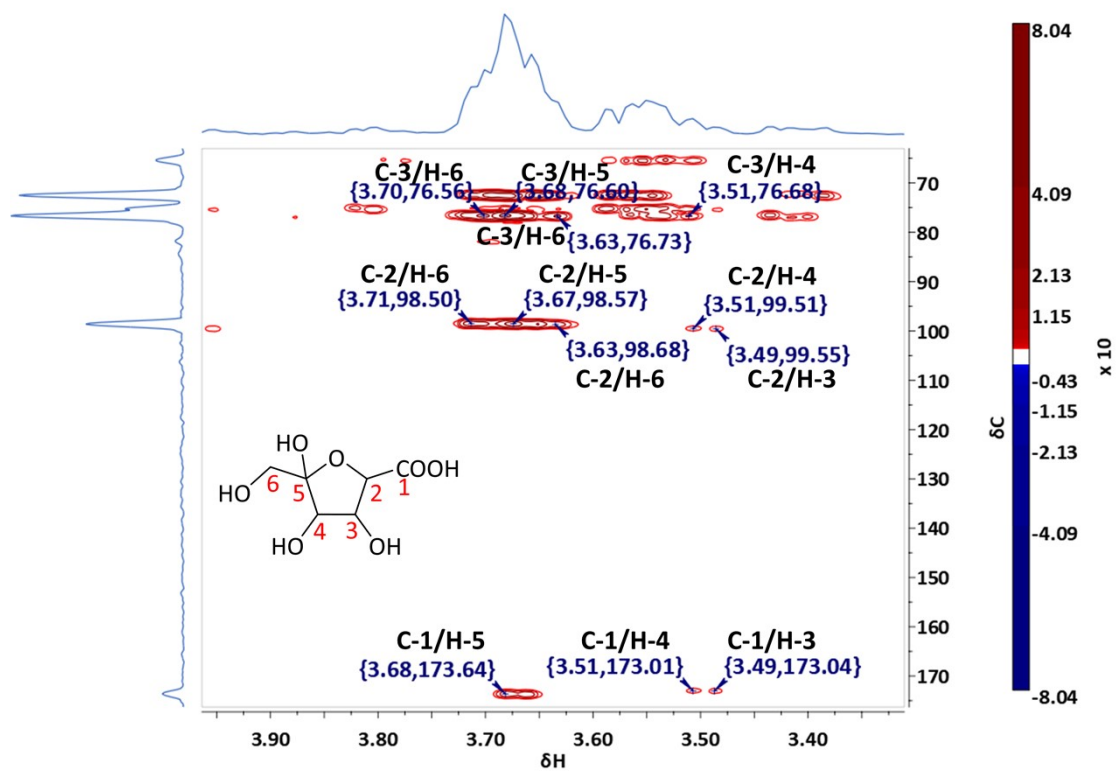
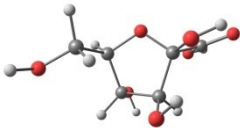
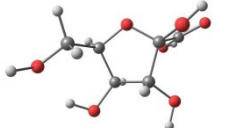
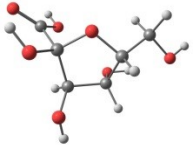
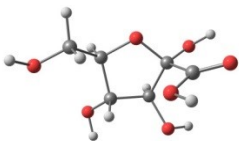




Table S8. Optimized geometries and energetic data of the A1-H isomers.

A1-H isomers	
	
$\Delta E_{A1-H} = 0.0$	$\Delta E_{A1-H-iso1} = 0.47$
	
$\Delta E_{A1-H-iso2} = 2.20$	$\Delta E_{A1-H-iso3} = 2.65$

Relative energy values are given in kcal/mol (color code, C: gray, H: white, O: red).

Fig. S16 Potential energy surface (PES) for Dehydrogenation of IM3-Me.

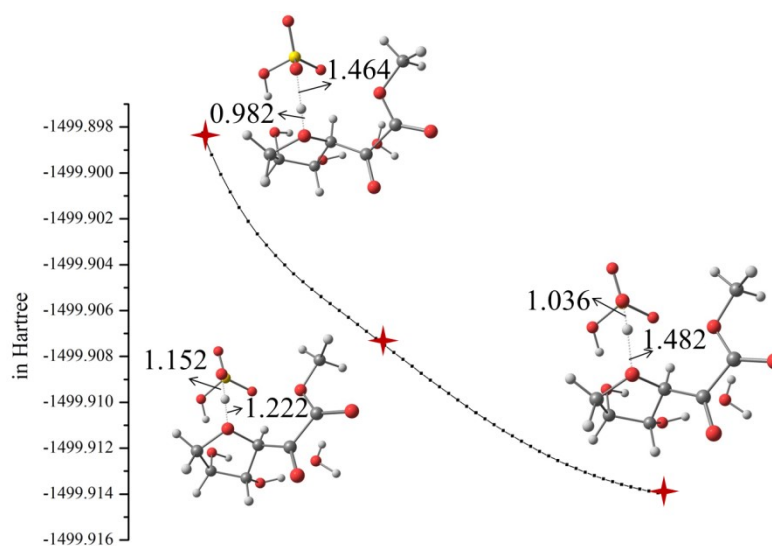
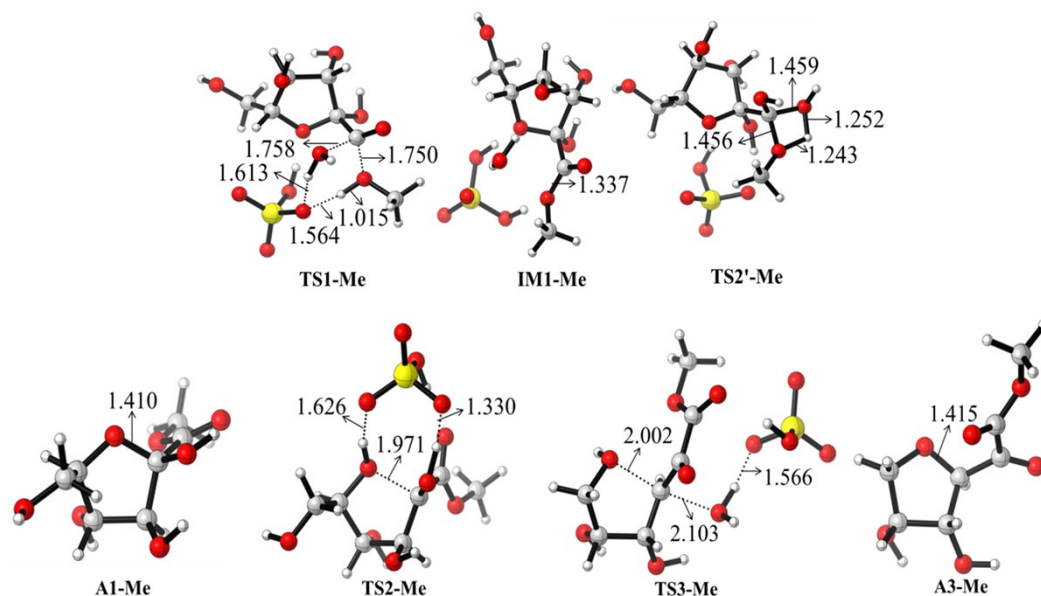


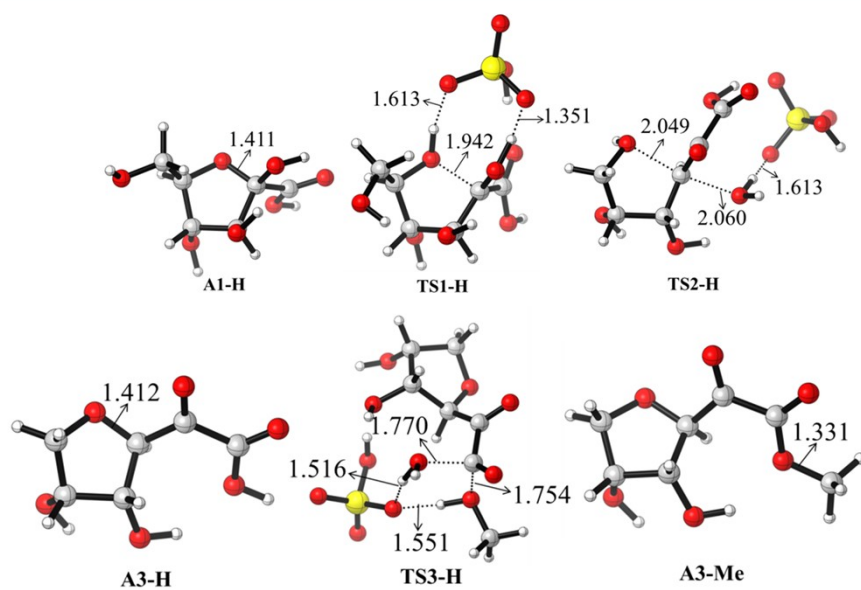
Fig. S16 Potential energy surface (PES) for Dehydrogenation of **IM3-Me**. Scanned by using O-H distance as reaction coordinate, along with some key optimized structures. The key bond distances in angstroms Å (color code, C: gray, H: white, O: red).

Fig. S17 The key bond distances in angstroms Å.



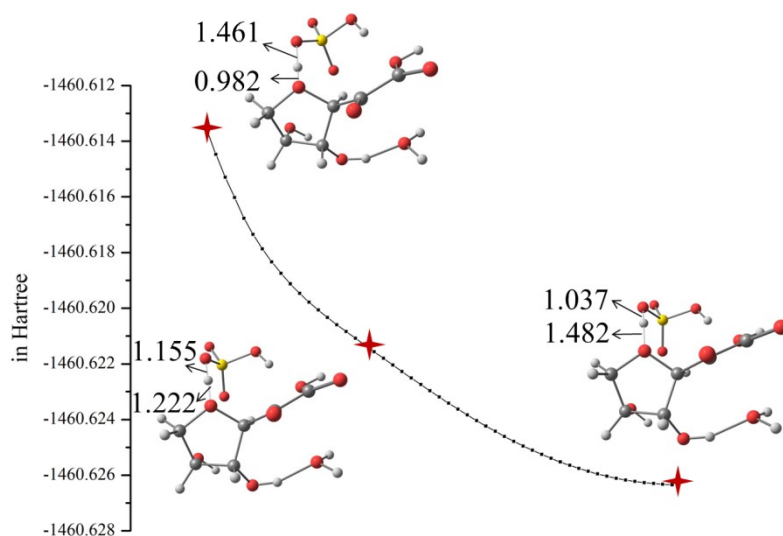
-Me

-H



Color code, C: gray, H: white, O: red.

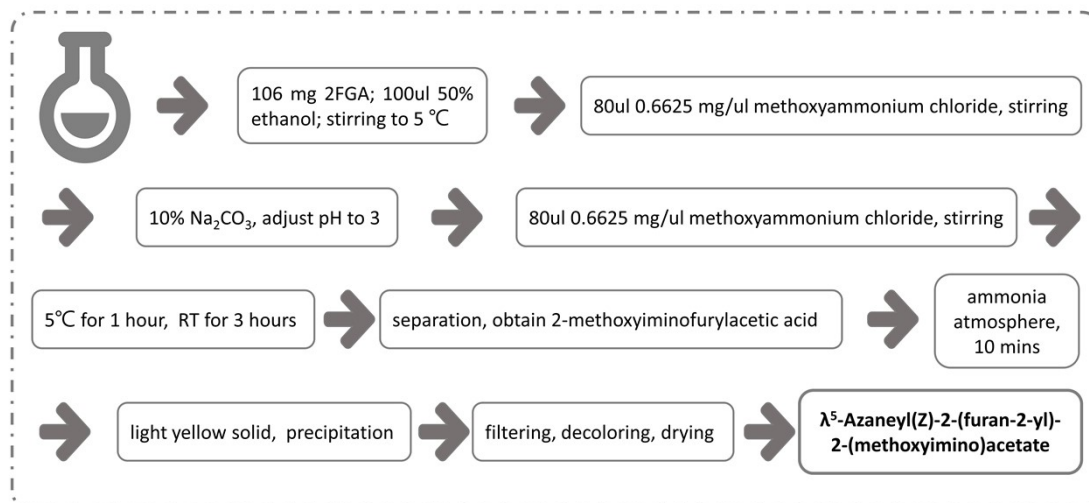
Fig. S18 Potential energy surface (PES) for Dehydrogenation of IM2-H.



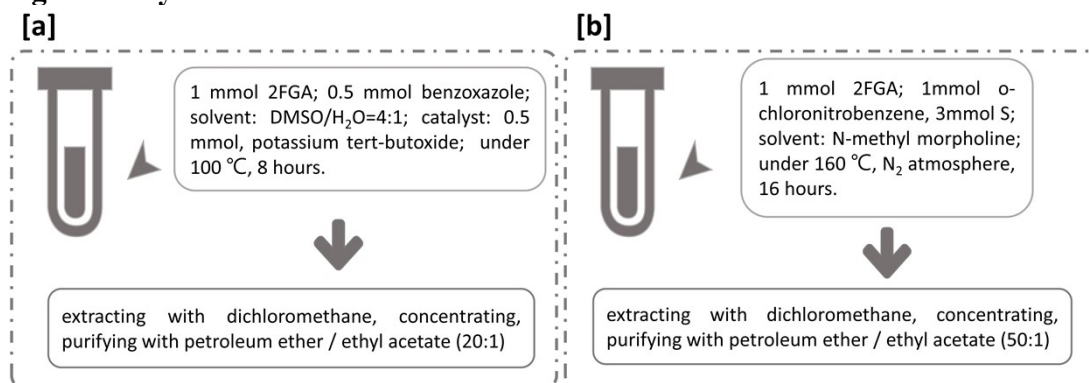
**Fig. S18** Potential energy surface (PES) for Dehydrogenation of **IM2-H**. Scanned by using O-H distance as reaction coordinate, along with some key optimized structures. The key bond distances in angstroms Å (color code, C: gray, H: white, O: red).

## General Method of derivations

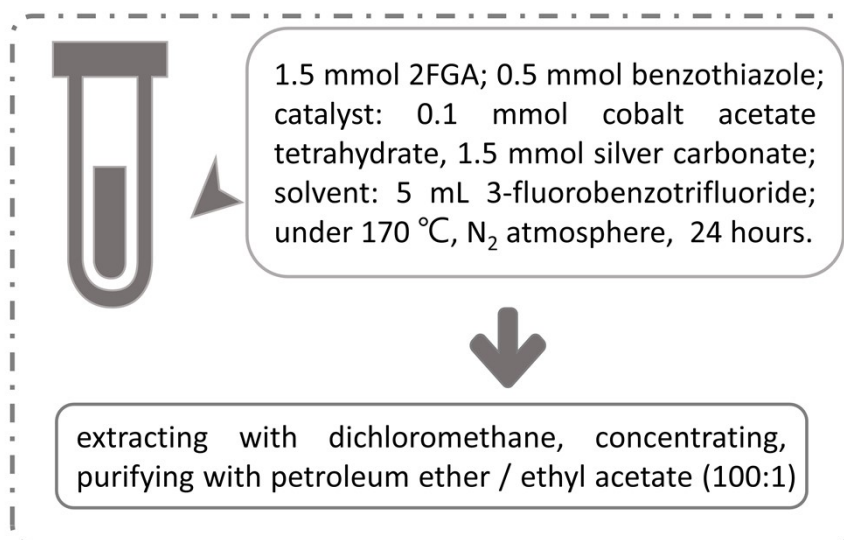
**Fig. S19 Synthesis of  $\lambda^5$ -Azaneyl(Z)-2-(furan-2-yl)-2-(methoxyimino)acetate.**



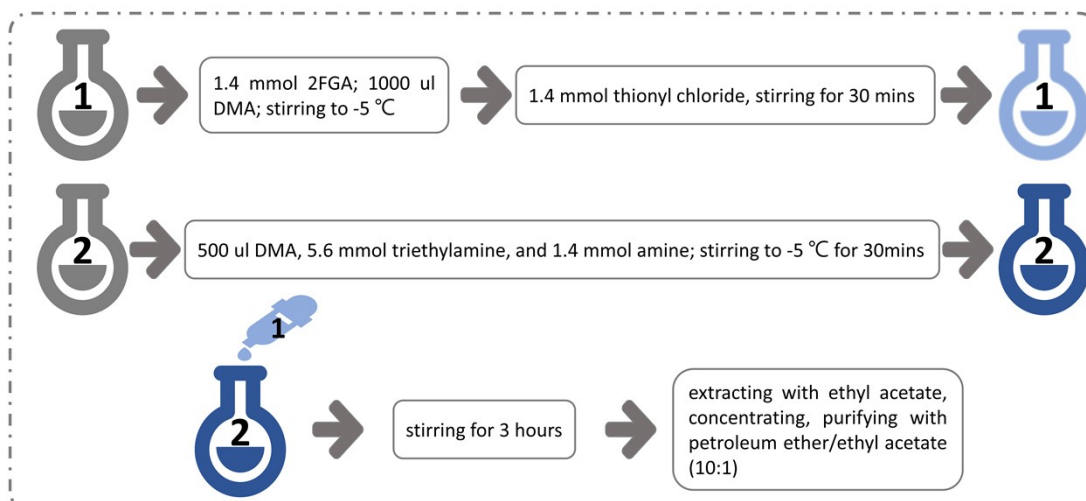
**Fig. S20 Aryl substitution.**



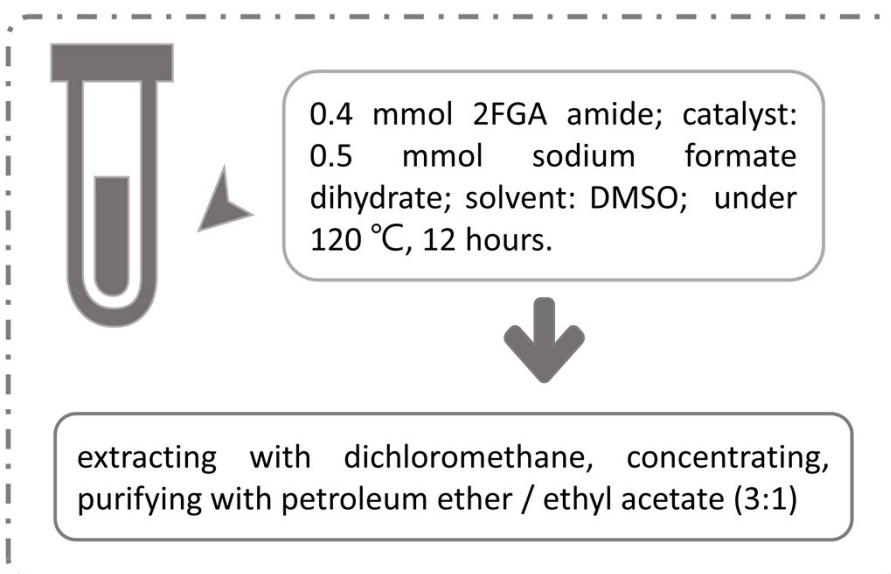
**Fig. S21 Decarboxylation coupling.**



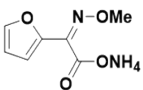
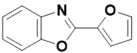
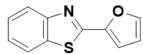
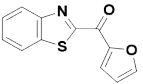
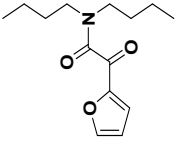
**Fig. S22 Amidation.**

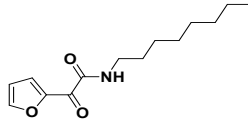
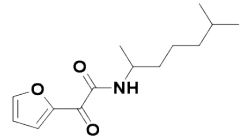
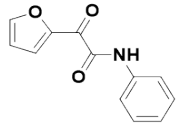
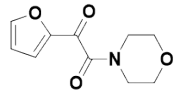
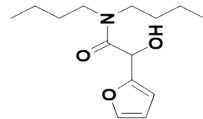


**Fig. S23 Amidation reduction.**



**Table. S9 Characterization of derivatives.**

Entry	Name & Yield [%]	Structure	Characterization of NMR
<b>1</b>	$\lambda$ 5-Azaneyl(Z)-2-(furan-2-yl)-2-(methoxyimino)acetate, <b>1d</b> <b>59</b>		$^{13}\text{C}$ NMR (126 MHz, DMSO) $\delta$ 164.48 (s), 150.51 (s), 147.76 (s), 143.97 (s), 111.43 (d, $J = 9.7$ Hz), 61.20 (s). $^1\text{H}$ NMR (500 MHz, DMSO) $\delta$ 7.60 (d, $J = 76.4$ Hz, 5H), 6.58 – 6.45 (m, 2H), 3.74 (s, 3H).
<b>2</b>	2-(Furan-2-yl)benzo[d]oxazole, <b>2d</b> <b>49</b>		$^{13}\text{C}$ NMR (101 MHz, $\text{CDCl}_3$ ) $\delta$ 155.27 (s), 150.14 (s), 145.70 (s), 142.62 (s), 141.63 (s), 125.25 (s), 124.82 (s), 120.12 (s), 114.24 (s), 112.22 (s), 110.53 (s), 77.32 (s), 77.00 (s), 76.68 (s). $^1\text{H}$ NMR (400 MHz, $\text{CDCl}_3$ ) $\delta$ 7.78 – 7.72 (m, 1H), 7.66 (dd, $J = 1.7, 0.7$ Hz, 1H), 7.58 – 7.53 (m, 1H), 7.38 – 7.32 (m, 2H), 7.27 (dd, $J = 3.5, 0.7$ Hz, 1H), 6.61 (dd, $J = 3.5, 1.8$ Hz, 1H).
<b>3</b>	2-(Furan-2-yl)benzo[d]thiazole, <b>3d</b> <b>34</b>		$^{13}\text{C}$ NMR (75 MHz, $\text{CDCl}_3$ ) $\delta$ 157.45 (s), 153.74 (s), 148.74 (s), 144.60 (s), 134.25 (s), 126.38 (s), 125.10 (s), 123.07 (s), 121.48 (s), 112.43 (s), 111.32 (s), 77.42 (s), 77.00 (s), 76.58 (s). $^1\text{H}$ NMR (300 MHz, $\text{CDCl}_3$ ) $\delta$ 8.05 (d, $J = 8.1$ Hz, 1H), 7.89 (d, $J = 7.9$ Hz, 1H), 7.61 (s, 1H), 7.49 (t, $J = 7.7$ Hz, 1H), 7.38 (t, $J = 7.6$ Hz, 1H), 7.19 (d, $J = 3.3$ Hz, 1H), 6.59 (s, 1H).
<b>4</b>	Benzo[d]thiazol-2-yl (furan-2-yl) methanone, <b>4d</b> <b>32</b>		$^{13}\text{C}$ NMR (126 MHz, $\text{CDCl}_3$ ) $\delta$ 153.66 (s), 125.99 (s), 125.37 (s), 123.50 (s), 121.71 (s), 76.78 (d, $J = 32.0$ Hz). $^1\text{H}$ NMR (500 MHz, $\text{CDCl}_3$ ) $\delta$ 8.98 (s, 1H), 8.13 (d, $J = 1.8$ Hz, 1H), 7.94 (s, 1H), 7.47 (d, $J = 42.5$ Hz, 2H).
<b>5</b>	2-(Furan-2-yl)-N-octyl-2-oxoacetamide, <b>5d</b> <b>54</b>		$^{13}\text{C}$ NMR (75 MHz, $\text{CDCl}_3$ ) $\delta$ 178.69 (s), 165.56 (s), 150.29 (s), 148.34 (s), 121.70 (s), 112.66 (s), 77.42 (s), 77.00 (s), 76.58 (s), 47.41 (s), 44.33 (s), 30.69 (s), 29.26 (s), 20.05 (s), 19.65 (s), 13.59 (d, $J = 17.8$ Hz). $^1\text{H}$ NMR (300 MHz, $\text{CDCl}_3$ ) $\delta$ 7.70 (s, 3H), 7.31 (d, $J = 3.6$ Hz, 3H), 6.60 (dd, $J = 3.5, 1.6$ Hz, 3H), 3.50 – 3.41 (m, 7H), 3.28 – 3.19 (m, 7H), 1.60 (qd, $J = 15.1, 7.5$ Hz, 15H), 1.40 (dq, $J = 14.0, 7.0$ Hz, 8H), 1.30 – 1.15 (m, 9H), 0.97 (t, $J = 7.3$ Hz, 11H), 0.85 (t, $J = 7.3$ Hz, 11H).

- 6** 2-(Furan-2-yl)-*N*-octyl-2-oxoacetamide, **6d**  
**54**
- 
- $^{13}\text{C}$  NMR (75 MHz,  $\text{CDCl}_3$ )  $\delta$  173.77 (s), 149.18 (s), 126.70 (s), 113.00 (s), 77.43 (s), 76.79 (d,  $J = 32.0$  Hz), 39.38 (s), 31.67 (s), 29.38 – 28.76 (m), 26.81 (s), 22.52 (s), 13.95 (s).  
 $^1\text{H}$  NMR (300 MHz,  $\text{CDCl}_3$ )  $\delta$  8.16 (d,  $J = 3.6$  Hz, 2H), 7.73 (s, 2H), 7.31 (s, 2H), 6.59 (dd,  $J = 3.5, 1.5$  Hz, 2H), 3.33 (dd,  $J = 13.7, 6.8$  Hz, 5H), 1.66 – 1.47 (m, 5H), 1.26 (d,  $J = 14.6$  Hz, 25H), 0.84 (t,  $J = 6.4$  Hz, 7H).
- 7** 2-(Furan-2-yl)-*N*-(6-methylheptan-2-yl)-2-oxoacetamide, **7d**  
**42**
- 
- $^{13}\text{C}$  NMR (126 MHz,  $\text{CDCl}_3$ )  $\delta$  173.72 (s), 160.10 (s), 149.45 (s), 149.15 (s), 126.66 (s), 112.94 (s), 77.26 (s), 77.00 (s), 76.75 (s), 42.19 (s), 39.25 (s), 30.87 (s), 28.72 (s), 24.14 (s), 22.80 (s), 13.86 (s), 10.70 (s).  
 $^1\text{H}$  NMR (500 MHz,  $\text{CDCl}_3$ )  $\delta$  8.14 (s, 1H), 7.71 (s, 1H), 6.57 (s, 1H), 3.26 (s, 2H), 1.50 (s, 1H), 1.36 – 1.17 (m, 8H), 0.86 (dd,  $J = 13.3, 5.8$  Hz, 6H).
- 8** 2-(Furan-2-yl)-2-oxo-*N*-phenylacetamide, **8d**  
**58**
- 
- $^{13}\text{C}$  NMR (75 MHz,  $\text{CDCl}_3$ )  $\delta$  173.46 (s), 157.56 (s), 149.59 (s), 136.40 (s), 129.12 (s), 127.23 (s), 125.27 (s), 119.93 (s), 113.22 (s), 77.99 – 77.53 (m), 77.42 (s), 76.79 (d,  $J = 32.2$  Hz).  
 $^1\text{H}$  NMR (300 MHz,  $\text{CDCl}_3$ )  $\delta$  9.12 (s, 1H), 8.26 (d,  $J = 3.3$  Hz, 1H), 7.88 – 7.62 (m, 3H), 7.37 (t,  $J = 7.7$  Hz, 2H), 7.17 (t,  $J = 7.3$  Hz, 1H), 6.64 (s, 1H).
- 9** 1-(Furan-2-yl)-2-morpholinoethane-1,2-dione, **9d**  
**58**
- 
- $^{13}\text{C}$  NMR (75 MHz, DMSO)  $\delta$  178.32 (s), 163.63 (s), 150.27 (s), 149.23 (s), 123.13 (s), 113.30 (s), 65.98 (s), 45.74 (s), 41.16 (s), 40.34 (s), 40.32 – 40.10 (m), 39.91 (d,  $J = 20.8$  Hz), 39.36 (d,  $J = 21.1$  Hz), 39.13 – 39.08 (m), 38.81 (d,  $J = 20.7$  Hz).  
 $^1\text{H}$  NMR (300 MHz, DMSO)  $\delta$  8.18 (d,  $J = 0.9$  Hz, 2H), 7.57 (d,  $J = 3.7$  Hz, 2H), 6.83 (dd,  $J = 3.7, 1.6$  Hz, 2H), 3.73 – 3.51 (m, 16H), 3.40 – 3.29 (m, 5H).
- 10** *N,N*-dibutyl-2-(furan-2-yl)-2-hydroxyacetamide, **10d**  
**75**
- 
- $^{13}\text{C}$  NMR (126 MHz,  $\text{CDCl}_3$ )  $\delta$  178.62 (s), 165.49 (s), 150.17 (s), 148.29 (s), 121.61 (s), 112.58 (s), 47.30 (s), 44.20 (s), 30.57 (s), 29.16 (s), 19.94 (s), 19.53 (s), 13.59 (s), 13.35 (s).  
 $^1\text{H}$  NMR (500 MHz,  $\text{CDCl}_3$ )  $\delta$  7.66 (s, 1H), 6.55 (s, 1H), 3.41 (s, 2H), 3.19 (s, 2H), 1.59 (s, 2H), 1.51 (s, 2H), 1.35 (d,  $J = 7.5$  Hz, 2H), 1.18 (d,  $J = 7.5$  Hz, 2H), 0.92 (s, 3H), 0.80 (s, 3H).

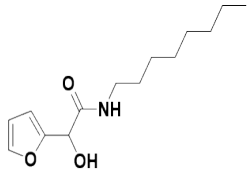
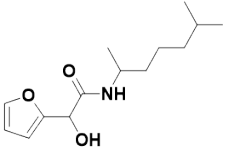
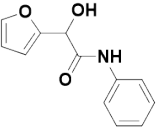
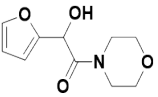
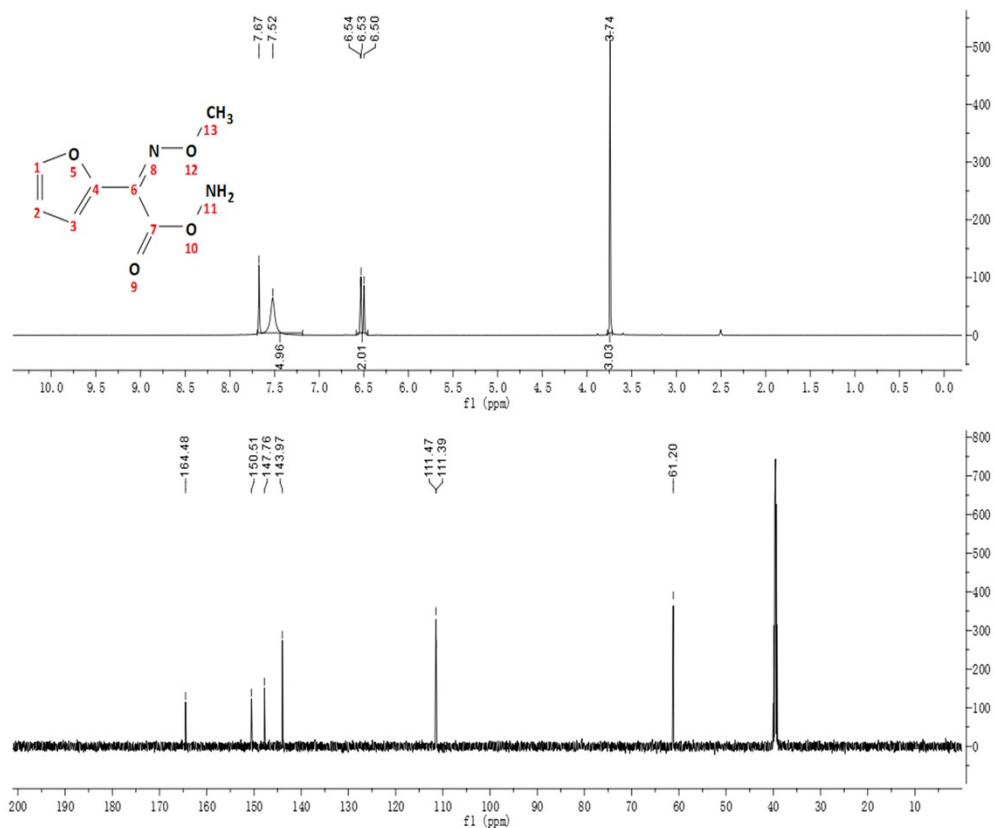
- 11** 2-(Furan-2-yl)-2-hydroxy-*N*-octylacetamide, **11d**  
**44**
- 
- $^{13}\text{C}$  NMR (126 MHz,  $\text{CDCl}_3$ )  $\delta$  173.68 (s), 159.92 (s), 149.11 (s), 126.65 (s), 112.93 (s), 39.29 (s), 31.59 (s), 28.97 (s), 26.73 (s), 22.44 (s), 13.88 (s).  
 $^1\text{H}$  NMR (500 MHz,  $\text{CDCl}_3$ )  $\delta$  8.16 (s, 1H), 7.73 (s, 1H), 6.60 (s, 1H), 3.33 (s, 2H), 1.57 (s, 2H), 1.24 (s, 10H), 0.85 (s, 3H).
- 12** 2-(Furan-2-yl)-2-hydroxy-*N*-(6-methylheptan-2-yl)acetamide, **12d**  
**37**
- 
- $^{13}\text{C}$  NMR (126 MHz,  $\text{CDCl}_3$ )  $\delta$  173.67 (s), 160.04 (s), 149.11 (s), 126.66 (s), 112.92 (s), 42.15 (s), 39.22 (s), 30.84 (s), 28.69 (s), 24.10 (s), 22.77 (s), 13.83 (s), 10.67 (s).  
 $^1\text{H}$  NMR (500 MHz,  $\text{CDCl}_3$ )  $\delta$  8.16 (s, 1H), 7.73 (s, 1H), 6.59 (s, 1H), 3.28 (s, 2H), 1.27 (s, 9H), 0.89 (s, 6H).
- 13** 2-(Furan-2-yl)-2-hydroxy-*N*-phenylacetamide, **13d**  
**90**
- 
- $^{13}\text{C}$  NMR (126 MHz,  $\text{CDCl}_3$ )  $\delta$  167.56 (s), 143.08 (s), 128.98 (s), 124.78 (s), 119.85 (s), 110.63 (s), 108.91 (s), 68.24 (s).  
 $^1\text{H}$  NMR (500 MHz,  $\text{CDCl}_3$ )  $\delta$  8.19 (s, 1H), 6.35 (d,  $J = 42.9$  Hz, 2H), 5.18 (s, 1H), 1.20 (s, 3H).
- 14** 2-(Furan-2-yl)-2-hydroxy-1-morpholinoethan-1-one, **14d**  
**77**
- 
- $^{13}\text{C}$  NMR (126 MHz, DMSO)  $\delta$  178.89 (s), 164.19 (s), 150.84 (s), 123.73 (s), 113.87 (s), 66.54 (s), 66.23 (s), 46.31 (s), 41.72 (s), 40.02 (s).  
 $^1\text{H}$  NMR (500 MHz, DMSO)  $\delta$  8.17 (s, 1H), 7.56 (s, 1H), 6.82 (s, 1H), 3.71 – 3.52 (m, 8H), 3.33 (d,  $J = 14.1$  Hz, 4H).
-

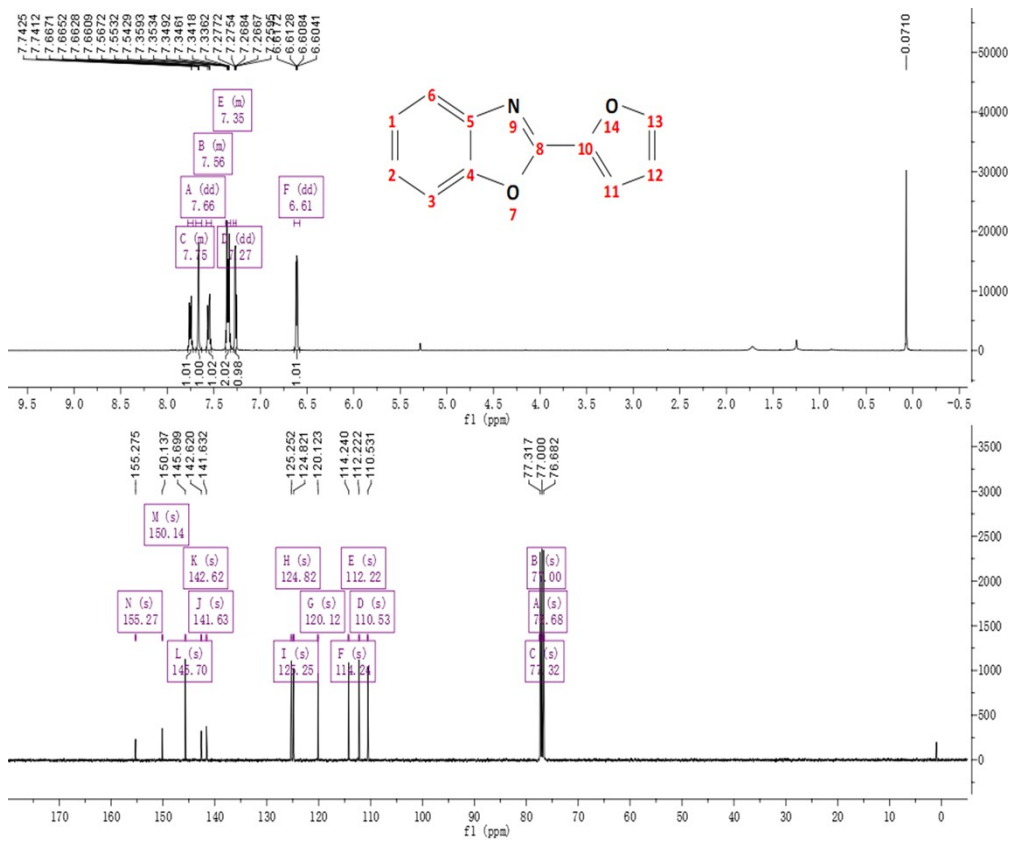


Fig. S24 <sup>1</sup>H and <sup>13</sup>C NMR Spectra of derivatives.

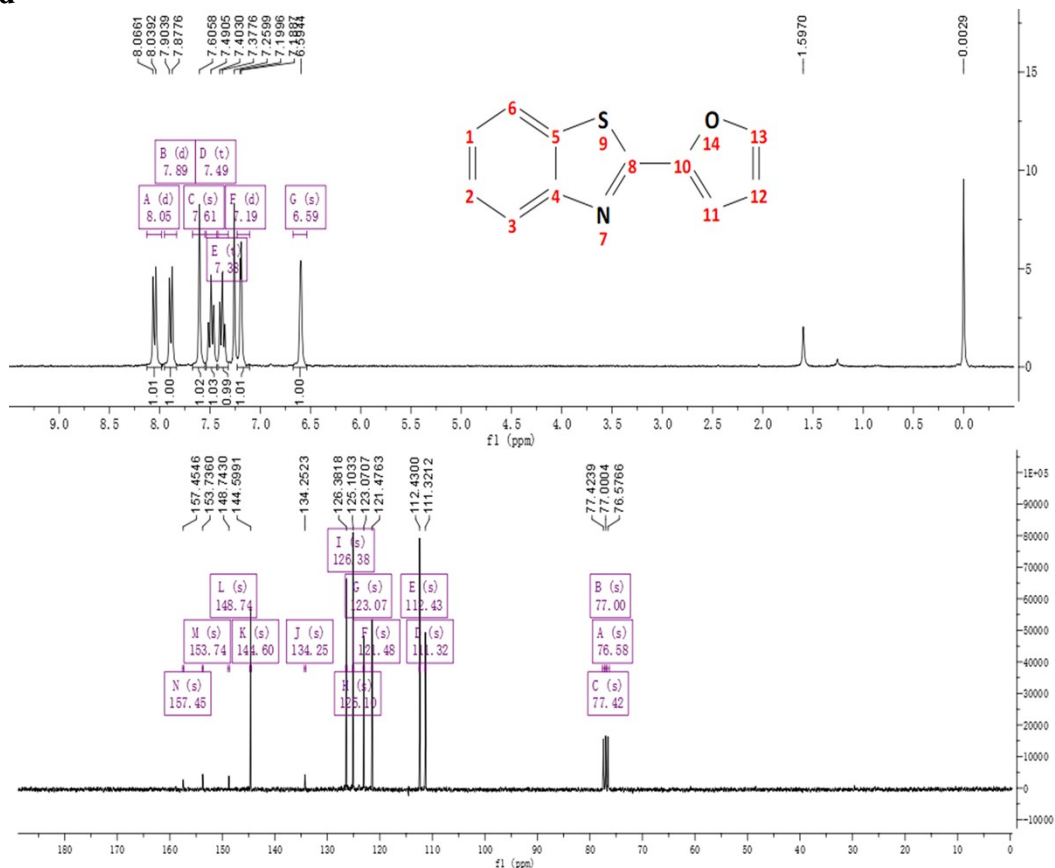
1d



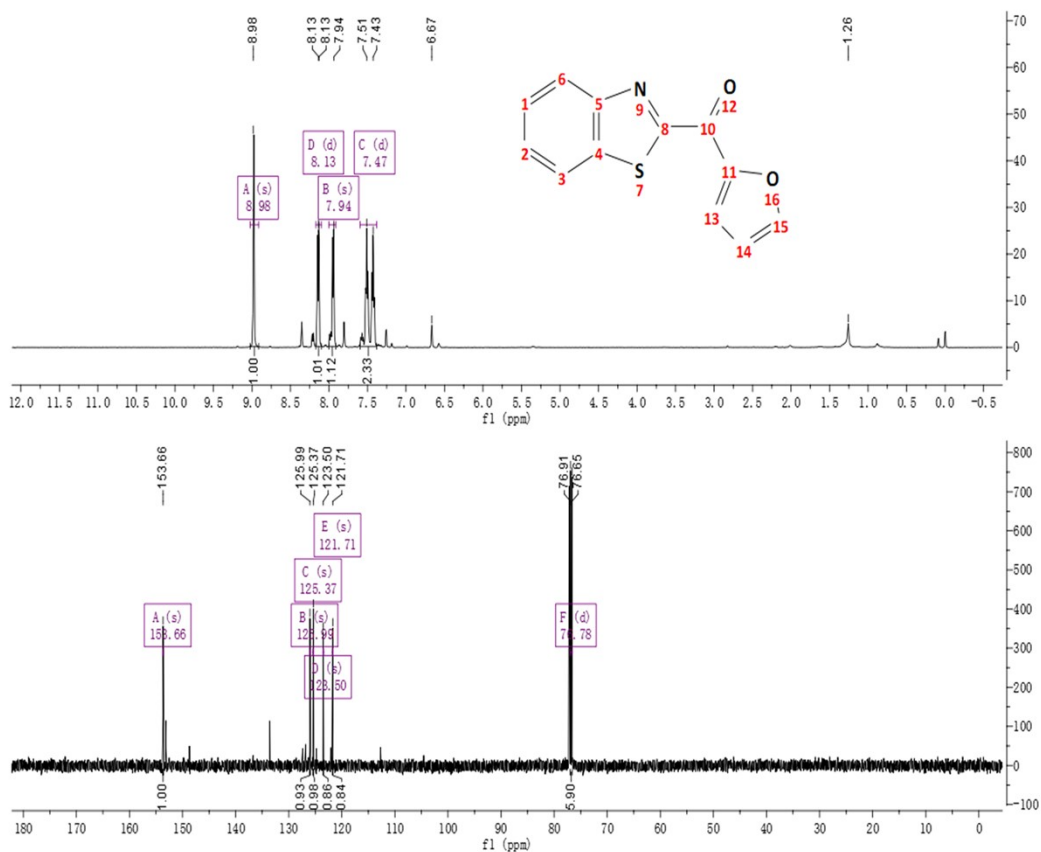
2d



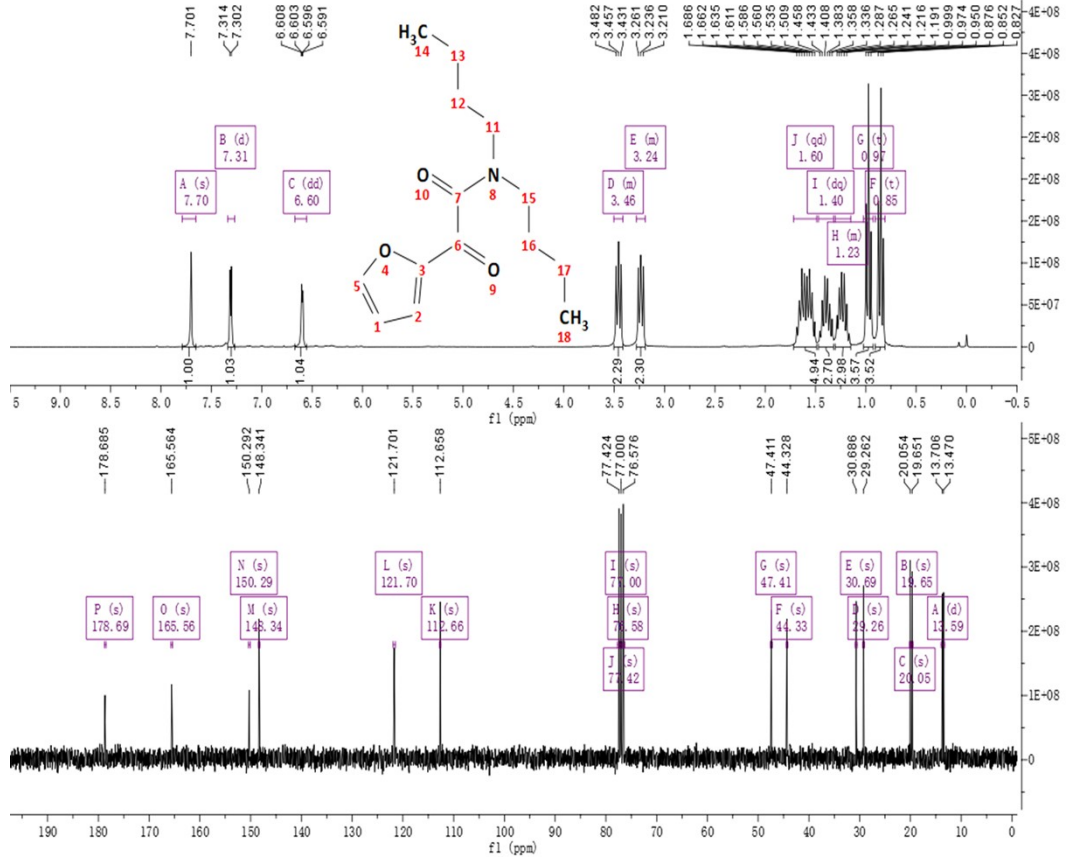
3d



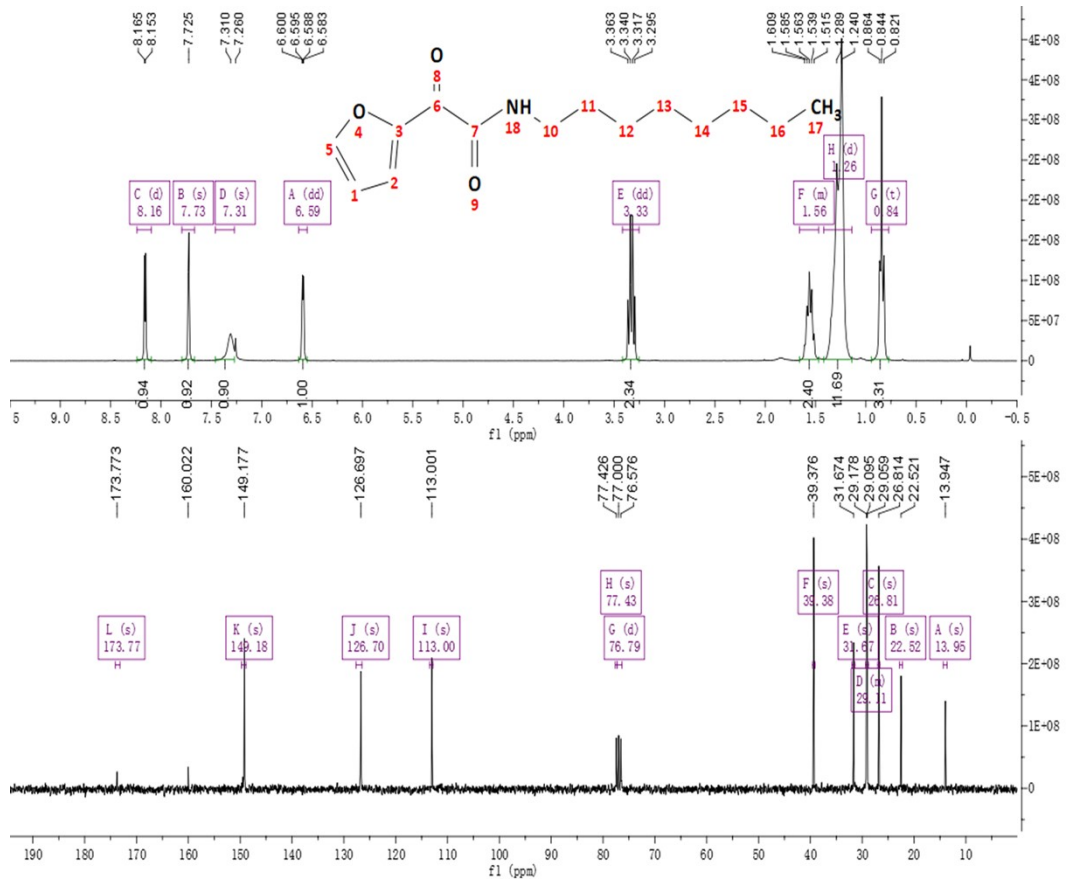
4d



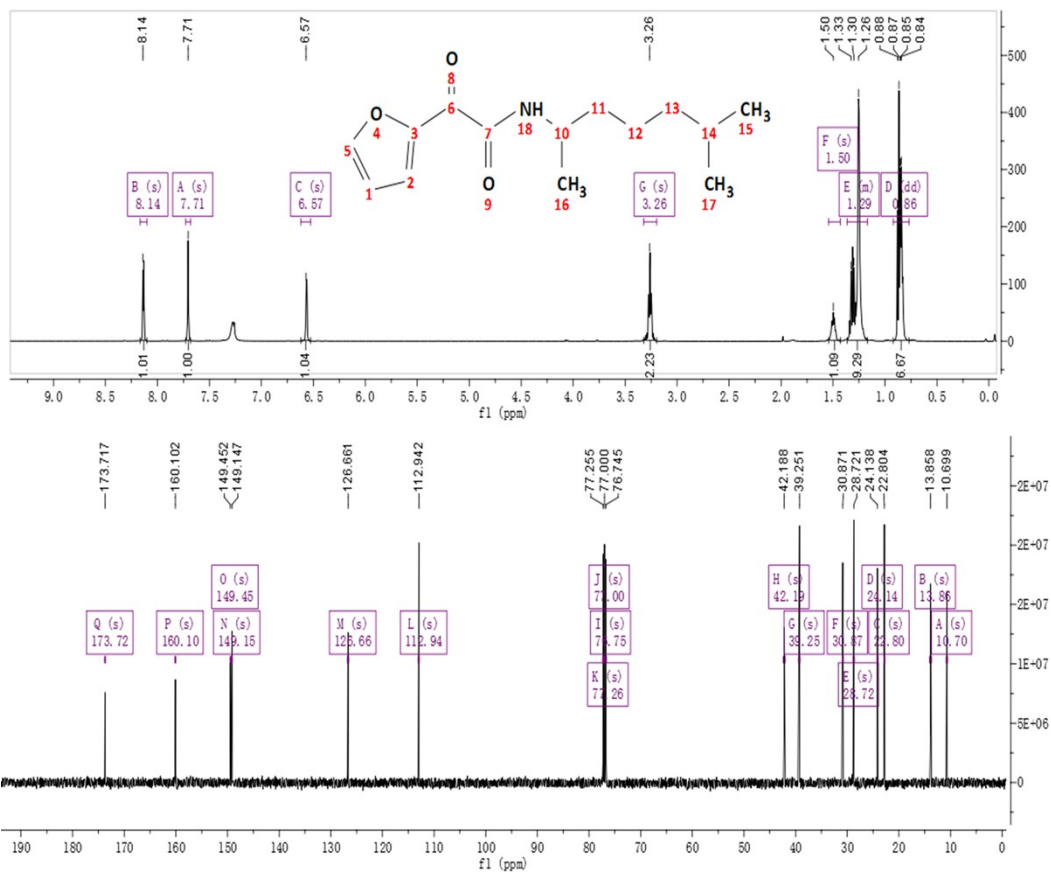
5d



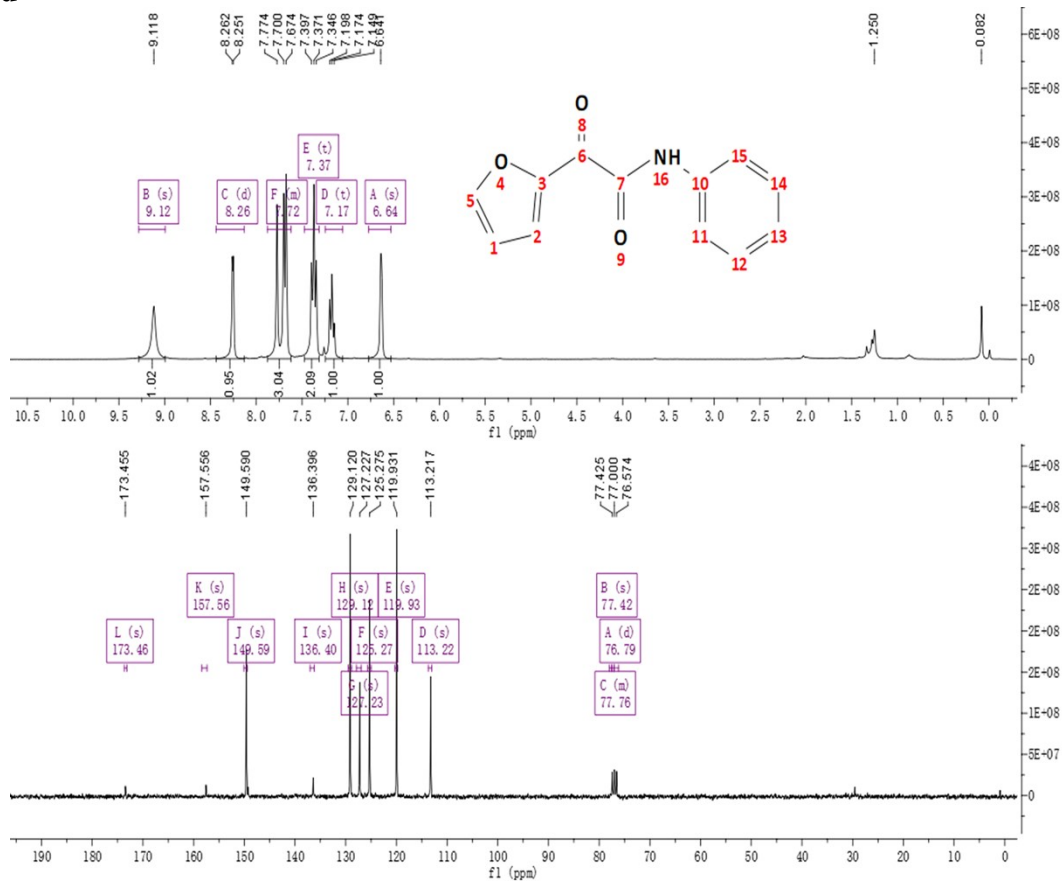
6d



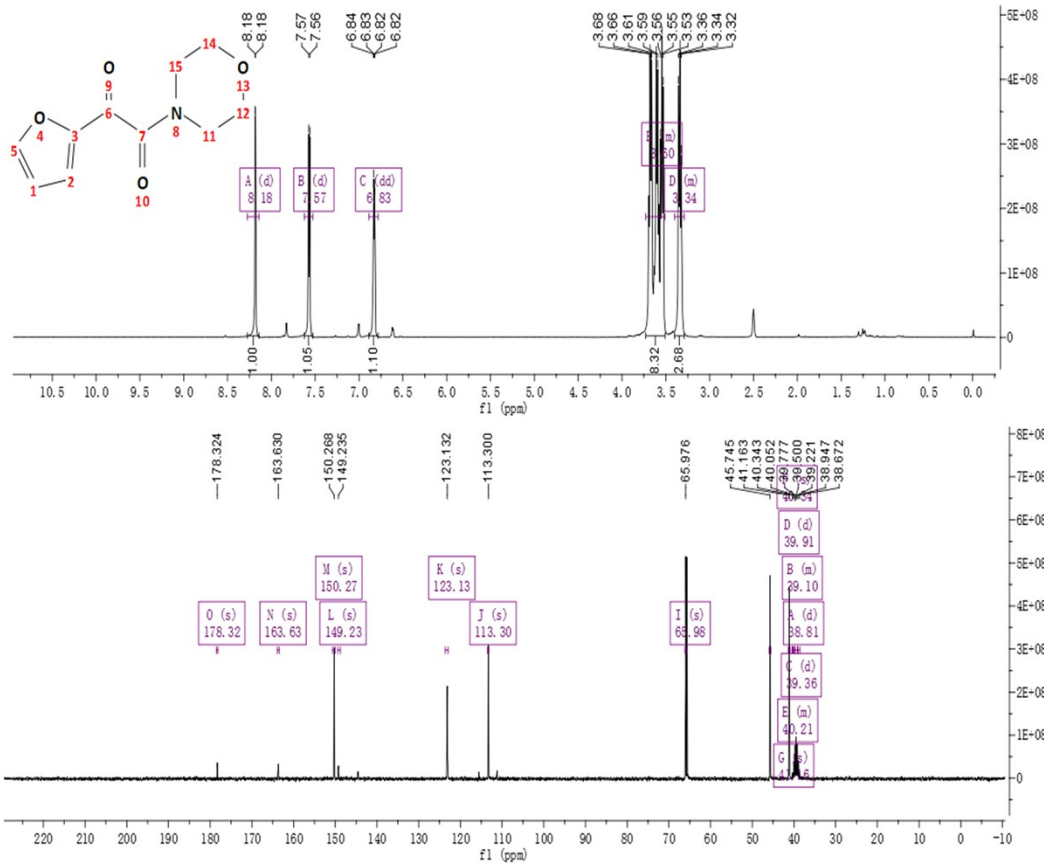
7d



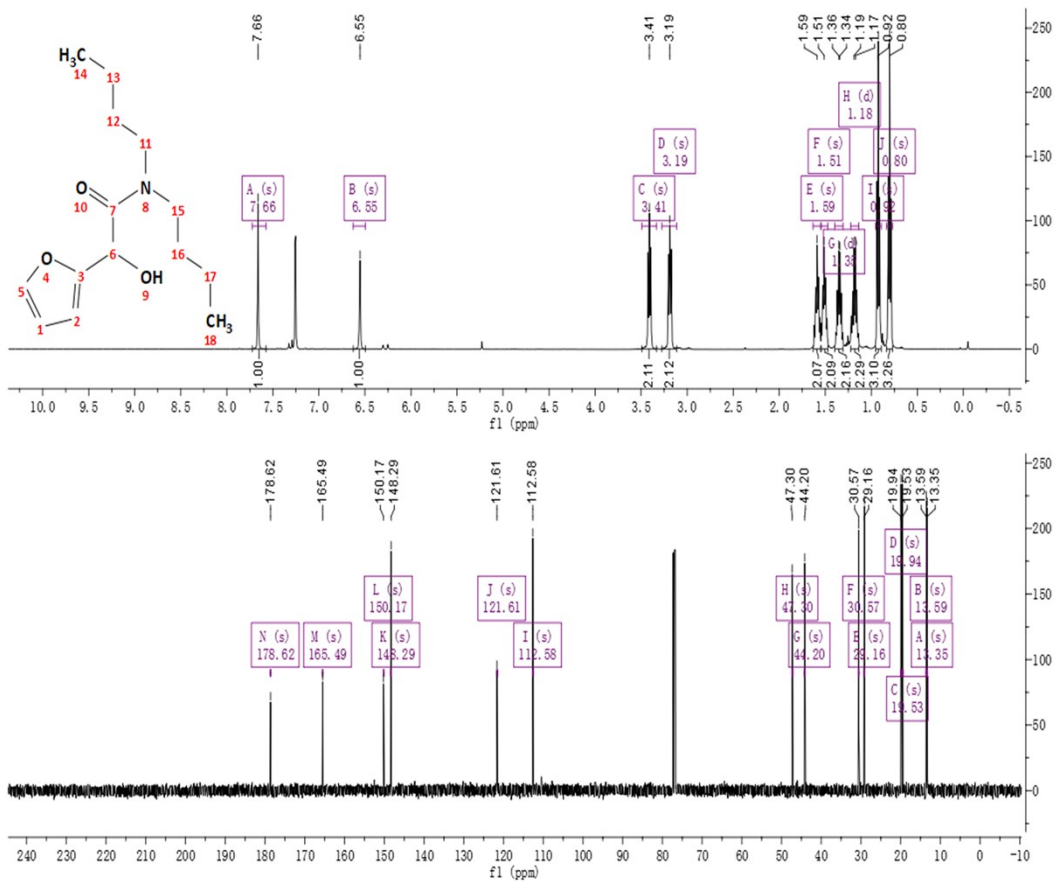
8d



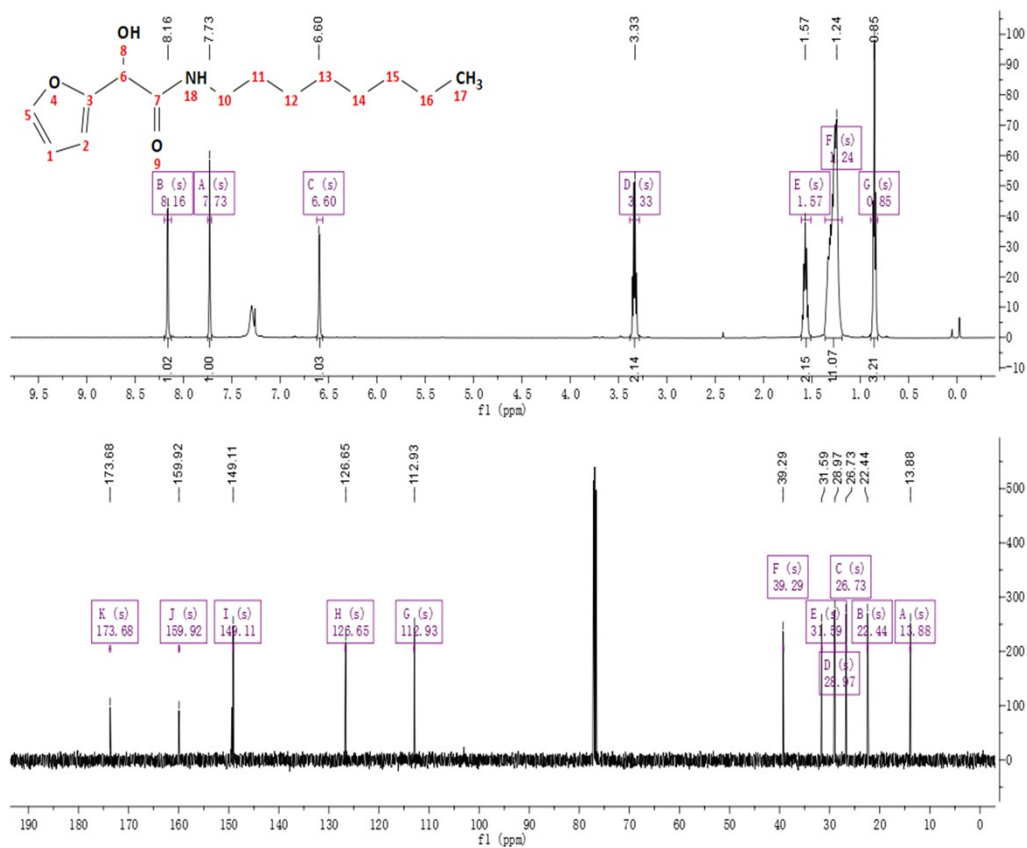
9d



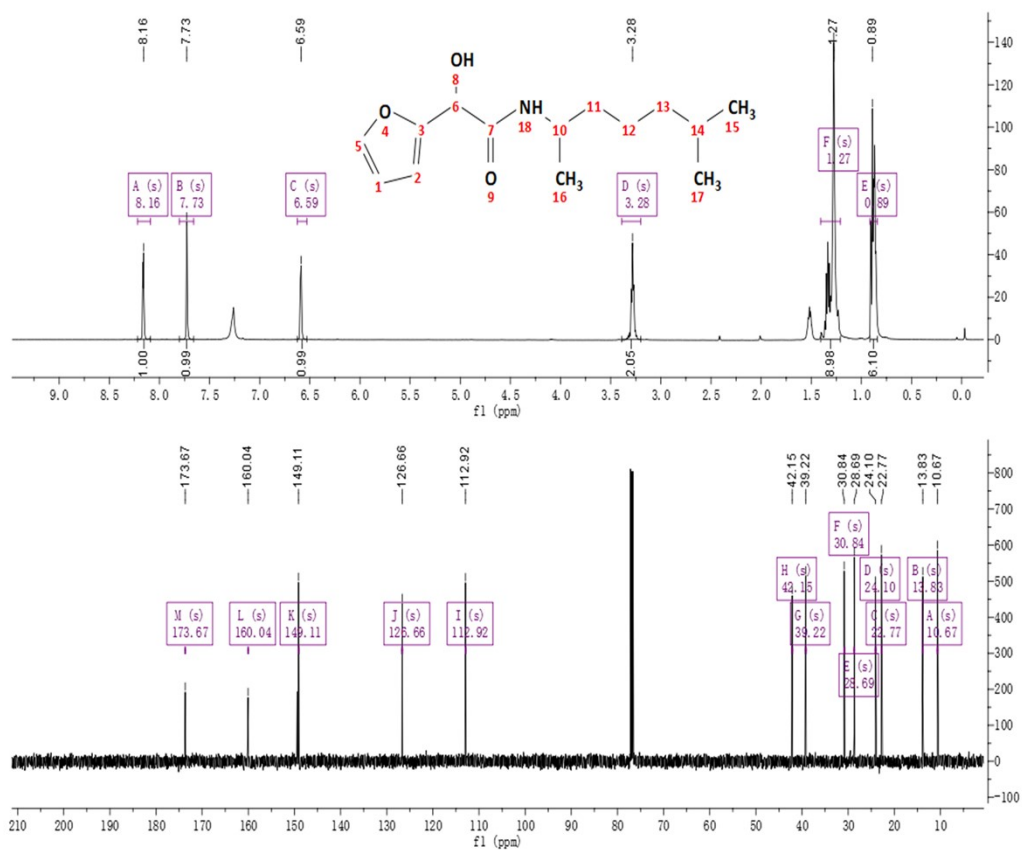
10d



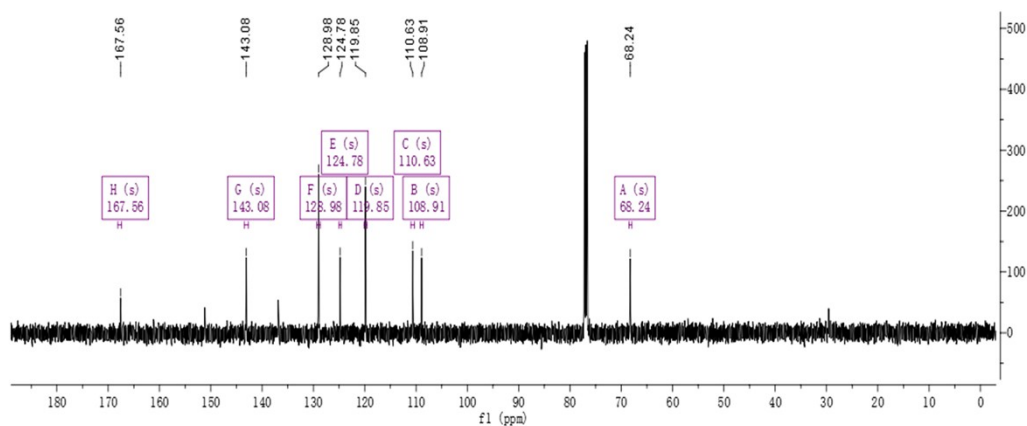
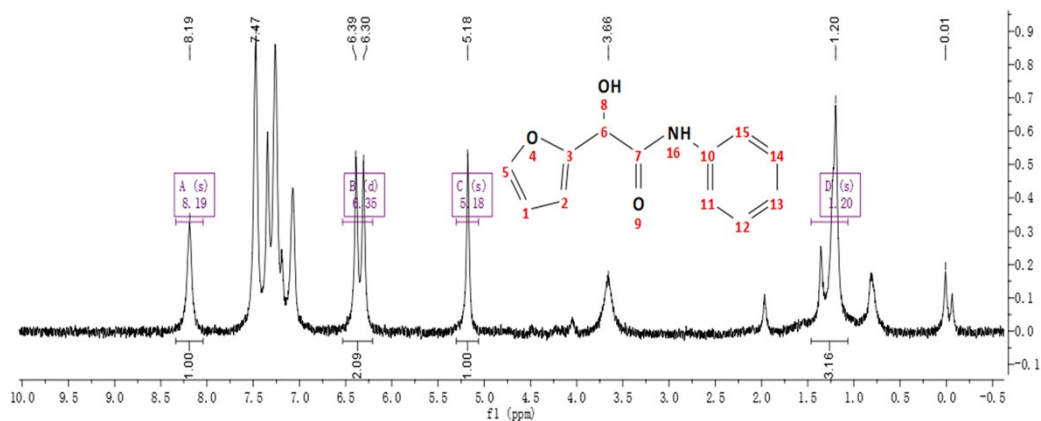
11d



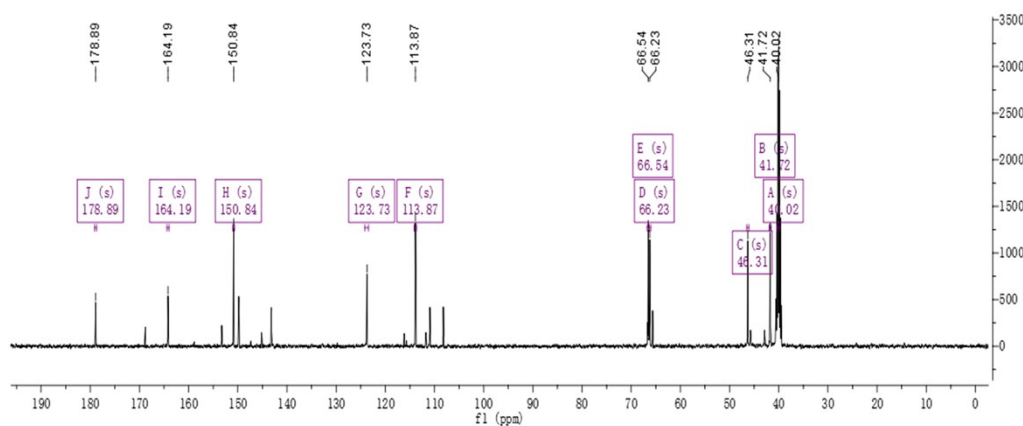
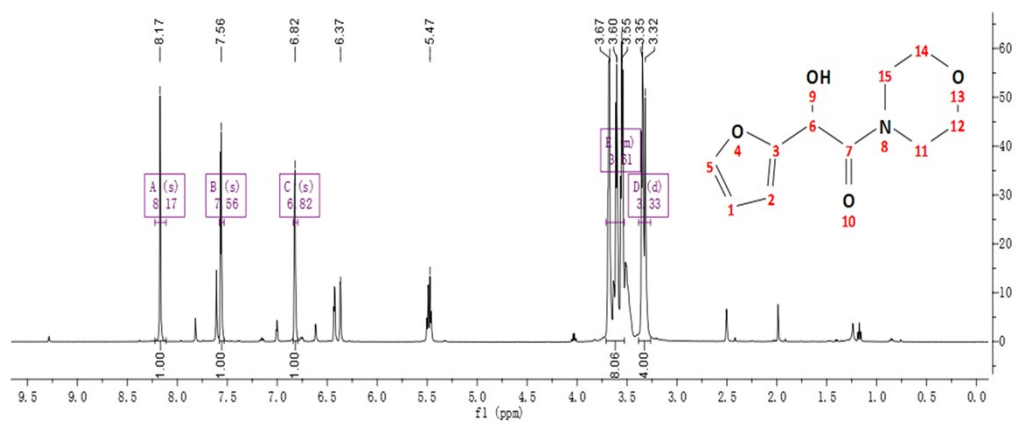
12d



13d



14d



# References

- 1 M. J. T. Frisch, G. W., H. B. Schlegel, G. E. Scuseria, M. A. C. Robb, J. R., G. Scalmani, V. Barone, Mennucci,, G. A. N. B., H. Petersson, M. Caricato, X. Li, Hratchian, H., A. F. B. P., J. Izmaylov, G. Zheng, J. L. Sonnenberg, M. Hada, K. M. T. Ehara, R. Fukuda, J. Hasegawa, M. Ishida, Y. T. H. Nakajima, O. Kitao, H. Nakai, T. Vreven, J. A. Montgomery, JR., J. E. Peralta, F. Ogliaro, M. Bearpark, J. J. B. Heyd, E., K. N. Kudin, V. N. Staroverov, Kobayashi,, J. R. R., K. Normand, A. Rendell, J. C. Burant, Iyengar,, J. C. S. S., M. Tomasi, N. Rega, J. M. Millam, M. Klene, Knox,, J. B. B. J. E., V. Cross, C. Adamo, J. Jaramillo, R. Gomperts, R. E. Y. Stratmann, O., A. J. Austin, R. Cammi, C. Pomelli, J. W. M. Ochterski, R. L., K. Morokuma, V. G. Zakrzewski, G. A. S. Voth, P., J. J. Dannenberg, S. Dapprich, Daniels, A., O. F. D., J. B. Farkas, J. V. Ortiz, J. Cioslowski and Fox, D. J. and R. A. G., *Gaussian 16, Inc.: Wallingford, CT*, 2016.
- 2 C. Lee, W. Yang and R. G. Parr, *Phys. Rev. B*, 1988, **37**, 785–789.
- 3 Y. Zhao and D. G. Truhlar, *Theor. Chem. Acc.*, 2008, **120**, 215–241.
- 4 F. Weigend, *PCCP*, 2006, **8**, 1057–1065.
- 5 F. Weigend and R. Ahlrichs, *PCCP*, 2005, **7**, 3297–3305.
- 6 S. Grimme, S. Ehrlich and L. Goerigk, *J. Comput. Chem.*, 2011, **32**, 1456–1465.
- 7 A. V. Marenich, C. J. Cramer and D. G. Truhlar, *J. Phys. Chem. B*, 2009, **113**, 6378–6396.
- 8 K. Fukui, *Acc Chem Res*, 1981, **14**, 363–368.
- 9 R. Krishnan, J. S. Binkley, R. Seeger and J. A. Pople, *J. Chem. Phys.*, 1980, **72**, 650–654.
- 10 O. V. Dolomanov, L. J. Bourhis, R. J. Gildea, J. A. K. Howard and H. Puschmann, *J. Appl. Crystallogr.*, 2009, **42**, 339–341.
- 11 G. M. Sheldrick, *Acta Crystallogr. C Struct. Chem.*, 2015, **71**, 3–8.